ECOLOGY

CO_2 leakage alters biogeochemical and ecological functions of submarine sands

Massimiliano Molari,[1]*† Katja Guilini,[2]† Christian Lott,[3] Miriam Weber,[1,3] Dirk de Beer,[4] Stefanie Meyer,[1‡] Alban Ramette,[1§] Gunter Wegener,[1,5] Frank Wenzhöfer,[1,6] Daniel Martin,[7] Tamara Cibic,[8] Cinzia De Vittor,[8] Ann Vanreusel,[2] Antje Boetius[1,5,6]

Subseabed CO_2 storage is considered a future climate change mitigation technology. We investigated the ecological consequences of CO_2 leakage for a marine benthic ecosystem. For the first time with a multidisciplinary integrated study, we tested hypotheses derived from a meta-analysis of previous experimental and in situ high-CO_2 impact studies. For this, we compared ecological functions of naturally CO_2-vented seafloor off the Mediterranean island Panarea (Tyrrhenian Sea, Italy) to those of nonvented sands, with a focus on biogeochemical processes and microbial and faunal community composition. High CO_2 fluxes (up to 4 to 7 mol CO_2 m^{-2} $hour^{-1}$) dissolved all sedimentary carbonate, and comigration of silicate and iron led to local increases of microphytobenthos productivity (+450%) and standing stocks (+300%). Despite the higher food availability, faunal biomass (−80%) and trophic diversity were substantially lower compared to those at the reference site. Bacterial communities were also structurally and functionally affected, most notably in the composition of heterotrophs and microbial sulfate reduction rates (−90%). The observed ecological effects of CO_2 leakage on submarine sands were reproduced with medium-term transplant experiments. This study assesses indicators of environmental impact by CO_2 leakage and finds that community compositions and important ecological functions are permanently altered under high CO_2.

INTRODUCTION

The atmosphere takes up large amounts of CO_2 from anthropogenic sources, resulting in global warming and increasing dissolution of CO_2 into seawater, with detrimental consequences for the ocean ecosystems (*1*). Ocean acidification is predicted to decrease seawater pH by 0.2 to 0.4 units by 2100 at unchanged rates of CO_2 emissions (*2*). To meet the international goal of limiting global warming to 1.5°C, the use of fossil fuels would have to end before 2040 (*3*) and may need to be complemented by mitigation technologies. One way to reduce industrial emissions is CO_2 capture and storage (CCS) in the subsurface, which includes subseabed reservoirs (*4*). This new maritime mitigation technology causes a need for assessments of ecological risk, especially from potential CO_2 leakage (*5*, *6*). Besides reducing effectiveness of the technology, CO_2 leakage from subseafloor reservoirs could lead to extreme pore- and seawater acidification, with pH substantially lower than 7 (*7*), and thereby negatively affecting the local ecosystem. Current knowledge of high-CO_2 effects on marine ecosystems is mostly based on assessing the vulnerability of individual specimens and mesocosm communities to artificially enhanced CO_2 levels in seawater (*8*, *9*). However, knowledge on long-term ecosystem-level responses and assessment of adaptation and resilience of communities are limited (*10*, *11*). Thus, a crucial question remains whether CO_2 leaks can locally lead to profound and persistent changes of element cycling, as well as to negative effects on ecosystem functions and services, including biodiversity and productivity. This question calls for field studies of naturally complex, dynamic ecosystems under long-term high-CO_2 exposure (for example, caused by volcanic degassing) (*12*, *13*). To our knowledge, this study is the first synchronous assessment (that is, occurring at the same time and place) of high-CO_2 effects covering all trophic levels from microbes to macrofauna in submarine sands. Sands make up a substantial proportion of shelf seas and play a critical role as biogeochemical filters at the land-sea boundary (*14*). We investigated for over 2 years the impact of CO_2 degassing on benthic biogeochemistry and community structure from microbes to macrofauna, focusing on carbon cycling (primary productivity and organic matter remineralization). In addition, we transplanted sediments between CO_2-vented and nonvented sites to assess the immediate effects of changing CO_2 levels within a year and to test whether we could reproduce the natural patterns. On the basis of a meta-analysis of previous high-CO_2 impact studies, we derived and tested the following hypothesis: CO_2 leakage enhances benthic primary production but negatively affects ecosystem functional diversity, with consequences for the benthic food web and carbon fluxes.

[1]HGF-MPG (Helmholtz Gemeinschaft Deutscher Forschungszenten–Max Planck Gesellschaft) Joint Research Group on Deep Sea Ecology and Technology, Max Planck Institute for Marine Microbiology, 28359 Bremen, Germany. [2]Marine Biology Research Group, Department of Biology, Ghent University, Ghent, Belgium. [3]HYDRA Institute for Marine Sciences, Elba Field Station, Via del Forno 80, 57034 Campo nell'Elba (LI), Italy. [4]Microsensor Group, Max Planck Institute for Marine Microbiology, 28359 Bremen, Germany. [5]MARUM, Center for Marine Environmental Sciences, University Bremen, 28359 Bremen, Germany. [6]HGF-MPG Joint Research Group on Deep Sea Ecology and Technology, Alfred Wegener Institute for Polar and Marine Research, Bremerhaven, Germany. [7]Centre d'Estudis Avançats de Blanes (CEAB), Consejo Superior de Investigaciones Científicas (CSIC), Blanes, Girona, Catalunya, Spain. [8]Sezione di Oceanografia, Istituto Nazionale di Oceanografia e di Geofisica Sperimentale – OGS, I-34151 Trieste, Italy.
*Corresponding author. Email: mamolari@mpi-bremen.de
†These authors contributed equally to this work.
‡Present address: University of Bergen, Bergen, Norway.
§Present address: Institute for Infectious Diseases, University of Bern, Bern, Switzerland.

RESULTS

Identification of natural analog sites for the leakage scenario

The Aeolian archipelago in the southern Tyrrhenian Sea is a ring-shaped volcanic arc (fig. S1A), composed of 7 islands and 10 seamounts, associated with the Peloritanian-Calabrian orogenic belt (*15*). Panarea, the smallest (3.3 km^2) Aeolian island, represents the emergent part of a wide stratovolcano more than 2000 m high and 20 km across (*16*). In 2011, we surveyed a number of CO_2-vented sites around Panarea to identify those to be used as "natural laboratories" to assess pure CO_2 effects, finally selecting the eastern side of Basiluzzo Islet (a rhyolitic dome northeast to Panarea). Two sites (fig. S1B) best fulfilled the "natural laboratory"

criteria: (i) continuous, dispersed degassing of CO_2 through sand causing low pH; (ii) similar oxygen availability and negligible coemission of toxic substances or microbial energy sources such as sulfide and methane; and (iii) no significant temperature anomalies from hydrothermalism. The selected "CO2-R" and "CO2-G" sites showed comparable environmental conditions to the reference (Table 1), and rather evenly distributed gas leakage (fig. S1D; density of two to three gas bubble strings per m^2). The reference site (REF) showed no gas emissions (fig. S1C).

Table 1. Main environmental characteristics of sampling sites at Basiluzzo Islet (Panarea Island, Italy). na, not available.

Site			REF	CO2-G	CO2-R
	Coordinates		N 38°39.827′	N 38°39.820′	N 38°39.749′
			E 15°07.118′	E 15°07.137′	E 15°07.123′
	Water depth	m	14–17	21	15–17
	Area†	m^2	100	35	200
	Seagrass meadows		*Posidonia oceanica*	*Posidonia oceanica*	*Posidonia oceanica*
Bottom water properties (10 cm asf)	Temperature‡	°C	18.8–19.5	18.8–19.0	18.7–19.3
	Salinity	‰	38	38	38
	O_2§,***	µmol liter^{-1}	243 (±9)	na	277 (±7)
	ORP§,***	mV	245 (±75)	na	133 (±64)
	pH_T¶		7.9	7.8	7.3
	DIC¶	mmol liter^{-1}	2.1 (±0.1)	2.3 (±0.1)	25 (±0.2)
	TA¶	mEq kg^{-1}	2.3 (±0.1)	2.3 (±0.1)	2.4 (±0.2)
	Ω_{calc}‖		4.0 (±0.2)	3.2 (±0.9)	1.3 (±0.6)
	$Si(OH)_4$††	µmol liter^{-1}	2.1 (±1.0)	2.7 (±1.8)	3.2 (±0.3)
	PO_4^{3-}††	µmol liter^{-1}	0	0.3‡‡	0
	NH_4††	µmol liter^{-1}	4.9 (±1.3)	1.8 (±1.5)	2.6 (±1.0)
	NO_2^-/NO_3^-††	µmol liter^{-1}	0.4 (±0.1)	0.8 (±0.4)	0.5 (±0.3)
	Fe††,*	µmol liter^{-1}	0.1 (±0.02)	0.2‡‡	0.7 (±0.1)
	Mn††	µmol liter^{-1}	0	0.5‡‡	0.4 (±0.1)
Sediment properties (0–10 cm layer)	Color		Gray	Gray	Red (rusty)
	Median grain size		Coarse sand	Coarse sand	Coarse sand
	Porosity§§	%	38–44	40–42	41–43
	Carbonate content¶¶,***	mg g^{-1}	9.34 (±1.13)	0.04 (±0.02)	0.08 (±0.02)
	Porewater pH_T‖‖		7.5–7.4	5.5–5.4	5.5
Porewater fluxes	Gas bubbling		No	Yes	Yes
	CO_2 content	%	—	90–97	97–99
	Gas flow†††	Liter m^{-2} hour^{-1}	—	80	120
	Porewater flow‡‡‡	Liter m^{-2} day^{-1}	11–69	12–45	11–85
	DIC flux§§§,***	mol m^{-2} day^{-1}	0.0–0.2	2.4–13.8	2.7–10.3
	$Si(OH)_4$§§§,***	mmol m^{-2} day^{-1}	0.0–0.9	10.0–41.7	17.6–28.2

†Patch of bare sediment within seagrass bushes. ‡Average temperatures in 2011 to 2013 measured in situ with SEAGUARD at 30 cm asf. §Average (±SD; n = 4000) of 2012 data collected in situ with RBR sensors over 15 days at 2 cm asf. ¶Average of 2011 to 2013 measurements (n = 9). ‖Calculated using R package seacarb v 3.0.11; input variables, pH_T and TA (for details, see table S1). ††Average (±SD; n = 3) of 2013 data; one sample available for PO_4^{3-}; one sample available for dissolved Fe and Mn at CO2-G. ‡‡No replicates available. §§Average porosity assessed from sediment samples collected in 2011 to 2013 (n = 3). ¶¶Average (±SD; n = 8) of $CaCO_3$ content in 0- to 2-cm and 4- to 6-cm layers for 2012 and 2013. ‖‖Average at top (0 to 2 cm) and bottom (8 to 10 cm) layers of sediment profile in 2011 to 2013 (for details, see table S1). †††At seafloor during low tide. ‡‡‡Range (2012 to 2013) of porewater efflux. §§§Range of fluxes measured in 2013 (n = 6). *P < 0.05, ***P < 0.001; Welch's t test between REF and CO2-R.

Gas and bottom water chemistry

The gas bubbles emanating at CO2-R and CO2-G consisted mainly of CO_2, with traces of CO and CH_4 (0.32 and 0.01 parts per million, respectively). Tidal variations in venting, with enhanced CO_2 leakage during low tide, caused peaks in pH_T (total scale; Fig. 1A). The CO_2 emission rates during low tide were 6.6 mol CO_2 m^{-2} $hour^{-1}$ at CO2-R and 4.2 mol CO_2 m^{-2} $hour^{-1}$ at CO2-G. Bottom water oxidation-reduction potential (ORP) at CO2-R was significantly lower than at REF (Table 1), being driven by effluxes of Fe^{2+}-enriched porewater at the vented sites (see section below). Bottom water O_2 concentration varied slightly with the light

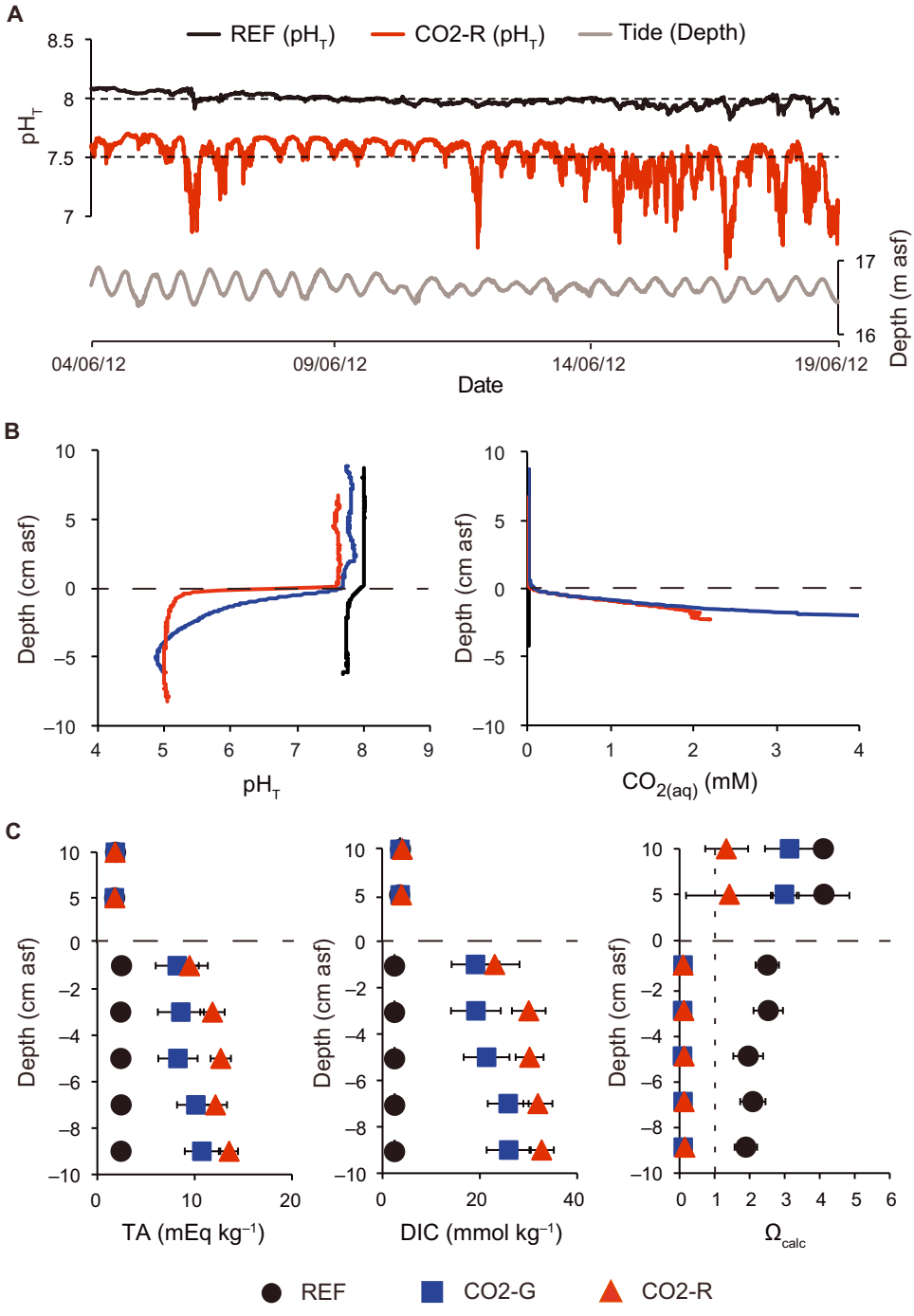

Fig. 1. Chemico-physical conditions. (**A**) Daily variation of bottom water pH_T over 15 days of in situ measurements with RBR sensors (dashed black line represents the average) at REF and CO2-R sites and the tide shown as variation in water depth (right *y* axis) of the CO2-R site in 2012. (**B**) Spatial variation of pH_T and dissolved CO_2 [$CO_{2(aq)}$] at REF, CO2-G, and CO2-R at high resolution below and above sediment surface (asf; spatial scale, 200 μm). The profiles were obtained with in situ microsensors in 2012. (**C**) Bottom water and porewater profiles for total alkalinity (TA), dissolved inorganic carbon (DIC), and saturation of calcite (Ω_{calc}); dashed line is the Ω_{calc} state threshold for carbonate dissolution. TA and DIC are average data (±SD; $n = 6$) of samples collected during campaigns 2012 to 2013. Ω_{calc} was calculated from pH_T and TA data.

period due to photosynthesis, with the average being higher at CO2-R than at REF (Table 1).

The bottom water pH_T measured at 5 to 10 cm above seafloor (asf) was, on average, 7.9 at REF and 6.6 to 7.7 at CO2-R (Fig. 2B), compared to 7.5 to 7.9 at CO2-G (table S1). Saturation states of calcite (Ω_{calc}) and aragonite (Ω_{ara}) were lower at the vented sites than at REF, but always >1 (Fig. 1C and table S1). Only marble tiles exposed to the vented seafloor partially dissolved within 1 year (n = 6; dissolution rates, 0.02 to 9.94 mg day^{-1}), whereas those with a distance >85 m away from the venting area center (CO2-R) did not show dissolution (n = 42). Nutrient levels (phosphate, ammonium, nitrite, and nitrate) in the bottom water did not differ significantly between the CO_2-impacted sites and REF (Table 1). The silicate content was also similar, with 1.2 to 1.8 µM in 2012 and 1.7 to 3.5 µM in 2013. However, iron and manganese bottom water concentrations increased at the CO_2-vented sites and were highest at CO2-R (Table 1).

Porewater chemistry

At REF, the pH_T decreased slightly with increasing sediment depth at REF, from 7.9 (sediment surface) to 7.7 [2.0 cm below seafloor (bsf)] and then remained constant (Fig. 1B and table S1). In contrast, at CO2-G and CO2-R, a pH_T of ca. 5.5 was reached already at 2.5 and 0.5 cm bsf, respectively (Fig. 1B and table S1). $CO_{2(aq)}$ increased rapidly with sediment depth, from 0.02 mM (sediment surface) to 5.3 mM (2 cm bsf) at both vented sites. O_2 penetrated to 2 cm bsf at REF and CO2-G sediments and to ca. 1 cm bsf at CO2-R (fig. S2A). ORP was constant at REF and decreased at CO2-G and CO2-R (to −50 mV within 1 cm bsf; fig S2A). No sulfide was detected in the subsurface porewaters, but peaks of a few micromolar were measured directly at the sediment surface at REF and CO2-G and to a lesser extent at ca. 0.5 cm bsf at CO2-R (fig. S2A). Hydrogen concentrations were below 1 µM (detection limit, 0.3 µM) and constant down to 5 cm bsf at all sites (fig. S2A). Together, the chemical gradients indicated that CO2-R was more strongly vented than CO2-G.

In REF sediments, porewater total alkali (TA) was constant but increased substantially with depth at the CO_2-vented sites (Fig. 1C). Ω_{calc} and Ω_{ara} decreased to <1 at the vented sites, whereas they remained around 2 and 1 at REF, respectively (Fig. 1C and table S1). Porewater at the vented sites was significantly enriched in silicate, iron, manganese, and, somewhat, phosphate (fig. S2B). Fe^{2+} was almost absent from REF porewaters, whereas it reached 0.5 to 1 mM at the vented sites, explaining the ORP dynamics in porewater and bottom waters and also the enhanced bottom water concentrations. In contrast, B, Ca, Na, Mg, Sr, Li, and K concentrations were similar at REF and CO_2-vented sites.

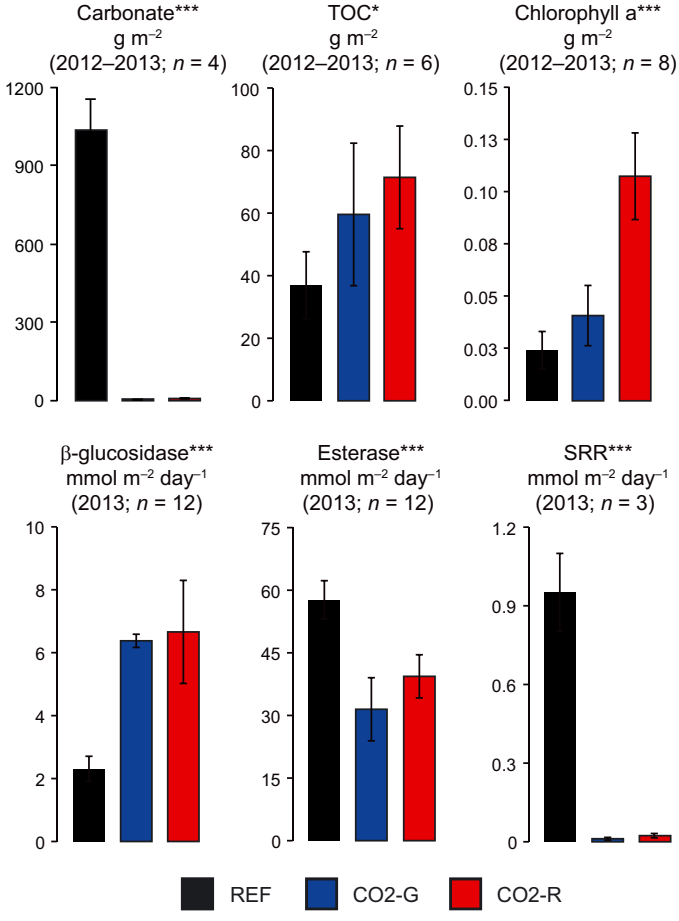

Fig. 2. Biogeochemical conditions at investigated sites. All data are integrated (summed up) over the 0- to 5-cm sediment layer, except for extracellular enzymatic activity (ß-glucosidase and esterase) data, which are integrated over the 0- to 2-cm layer (error bars are ±SD; year and number of sampling are given in each plot). TOC, total organic carbon; SRRs, sulfate reduction rates. Stars indicate significant differences between sites [analysis of variance (ANOVA); *P < 0.05, ***P < 0.001; for details, see table S2C].

Sediment grain size, carbonate, and elemental composition

All three sites were dominated by coarse sand with similar porosity and grain size distribution (Table 1). Concurrent with the observed undersaturation in calcite and aragonite in porewaters of the vented sites, the solid-phase carbonate content was about 100 to 200 times lower compared to those in REF sediments (Table 1 and Fig. 2). In accordance with the high porewater Fe concentration, also solid Fe was elevated at the vented sites (3.4 mg g^{-1} at CO2-R versus 0.4 mg g^{-1} at REF). Total organic carbon (TOC) was low (<0.1%) but approximately twofold higher in the surface sediments of CO2-R and CO2-G compared to REF (Fig. 2). Total organic nitrogen (TN) was also very low (<0.2 µg mg^{-1}) at all three sites, leading to a C/N ratio of ca. 4 to 7.5 in the surface sediments. Both TOC and TN were higher in 2013 than in 2012 (table S2A).

Fluxes and remineralization rates

Benthic chambers placed in between the bubble streams at the CO_2-vented sites showed a decreasing pH in the enclosed water bodies with time, together with a substantial efflux of dissolved organic carbon (DIC) and silicate from the sediment (table S3). In comparison, at REF, no effluxes of silicate or DIC were detected, and the chamber water pH_T remained stable at 8.0 in incubations of up to 5 hours.

Benthic chamber measurements at the vented sites showed similar advective fluid flow rates as those at REF (Table 1). On the basis of ORP signals, porewater iron concentrations, and fluid flow rates, it is likely that a substantial iron efflux occurred at the vented sites. Thus, respiration rates were corrected for potential oxygen consumption by purely chemical Fe^{2+} oxidation, which amounted to 1 to 7% of the total oxygen consumption at the vented sites. At the time of chamber deployments, the seafloor at all sites showed net oxygen consumption, and respiration always exceeded photosynthetic O_2 production even during daytime. However, both oxygen respiration and production were substantially higher at the vented sites compared to REF (Table 2). Diffusive oxygen fluxes calculated from microprofiler measurements (fig. S2) were <10% of the total fluxes but were also higher at CO2-R (2.6 mmol m^{-2} day^{-1}) than at REF (1.7 mmol m^{-2} day^{-1}).

Table 2. Benthic oxygen fluxes. Oxygen exchange (transparent chamber; net O_2 flux), oxygen respiration (masked chamber; O_2 respiration), and oxygen production [GPP = net O_2 flux + (O_2 respiration)] rates obtained from benthic chambers deployed in 2013; oxygen production–to–respiration (GPP/R) ratio, respiration per unit of total biomass (R/B_{Total}), and respiration per unit of heterotroph biomass (bacteria and animals; $R/B_{Heterotrophs}$). Benthic masked chambers rates (n = 2) and average (mean with ±SD in parenthesis), maximum (Max), and minimum (Min) rates of transparent chambers (n = 3 to 4) and O_2 production (n = 6 to 8) are given. nt, not tested for significance level; ns, not significant ($P > 0.05$).

		Net O_2 flux (daylight)^{ns}	O_2 respiration (masked)^{nt}	O_2 production**	GPP/R	R/B_{Total}	$R/B_{Heterotrophs}$
		mmol m^{-2} day^{-1}	mmol m^{-2} day^{-1}	mmol m^{-2} day^{-1}		day^{-1}	day^{-1}
REF	Mean	−7 (6)	na	10 (8)†	0.6	0.06/0.14	0.07/0.18
	Max	−11	−23	21			
	Min	−2	−10	0			
CO2-G	Mean	−58 (63)	−188‡	130 (63)	0.7	1.13	2.06
	Max	−151	na	173			
	Min	−15	na	37			
CO2-R	Mean	−18 (6)	na	55 (37)§	0.8	0.16/0.49	0.41/1.14
	Max	−24	−106	96			
	Min	−11	−38	15			

†Average (±SD; n = 6) of O_2 production calculated from each Net O_2 flux using O_2 respiration from both masked chambers. ‡At CO2-R, only one masked chamber was available. §Average (±SD; n = 8) of O_2 production calculated from each O_2 flux using O_2 respiration from both masked chambers. **$P < 0.01$ (Welch's t test between REF and CO2-R).

Standard proxies for microbial activities were also influenced by high CO_2. The β-glucosidase hydrolytic activity measured at substrate saturation (V_{max}) was significantly higher at CO2-G and CO2-R than at REF, whereas the aminopeptidase and esterase activities were significantly lower at the vented sites (Fig. 2 and fig. S3). No significant differences between sites were observed in chitobiase activity (fig. S3). SRRs determined in vitro were substantially higher at REF than at both vent sites (Fig. 2). Its contribution to aerobic benthic respiration was 16% at REF and 0.04% at the vent sites.

Microbial community patterns

Benthic diatoms (Bacillariophyceae) dominated the microphytobenthos in the surface sediment layer (95 ± 4% of cells), and their abundances were up to three times higher at CO2-R than at CO2-G and REF. Abundances were ca. 50% lower in 2012 than in 2013 at all sites: 4709 ± 636 cells cm^{-2} and 8932 ± 560 cells cm^{-2} at CO2-R, 1552 ± 158 cells cm^{-2} and 6079 ± 973 cells cm^{-2} at CO2-G, and 1744 ± 150 cells cm^{-2} and 4909 ± 218 cells cm^{-2} at REF, respectively (table S2A). CO2-R also showed the highest content of chlorophyll a (Chl a) pigments (Fig. 2). Chl a made up 73 to 95% of the chloroplastic pigment equivalents (CPEs), indicating that the pigments originated mostly from living cells. At all sites, Chl a decreased with sediment depth, with 33 to 50% concentrated in the top 2 cm, and was positively correlated with TOC (Pearson's $R = 0.4967$; $P < 0.001$; $n = 63$).

In contrast, total bacterial cell abundances were similar at all sites (Fig. 3A). The highest abundances occurred in the upper sediment layer (ca. 0.7×10^9 cells ml^{-1}) and decreased with sediment depth. Bacteria dominated [54 to 71% of 4′,6-diamidino-2-phenylindole (DAPI)–stained cells] over Archaea (3 to 1% of DAPI-stained cells).

With 454 massively parallel tag sequencing (MPTS), we recovered a total of 9674 bacterial operational taxonomic units ($OTUs_{0.03}$) from all sediment layers combined. At the class level, bacterial communities of the vented sites were dominated by Flavobacteria, Gammaproteobacteria, Deltaproteobacteria, Caldilinaea, and unclassified Cyanobacteria (Fig. 3A). Functional group analysis (table S4) showed that CO_2 leakage stimulated primary producers (that is, Cyanobacteria and Chlorobia), aerobic and anaerobic organic matter–degrading bacteria (that is, Flavobacteria and Caldilineae), some metal-reducing bacteria (that is, Desulfuromonadales), and some ferrotrophic bacteria (that is, Rhodobacteraceae). Concurrent with the negative impact of high CO_2 on SRR, the relative sequence abundances of sulfate reducers (that is, Desulfobacterales) were reduced, as well as those of sulfur oxidizers (that is, *Candidatus Thiobios*) and nitrifiers (that is, *Nitrospira*, *Nitrosospira*, and *Nitrosococcus*).

pH and DIC were the main environmental parameters influencing the bacterial community structure, explaining more than 35% of the variance in OTU composition for all data sets [that is, amplified ribosomal intergenic spacer analysis (ARISA) and MPTS; table S5A]. The three sites differed in bacterial community composition by 58 to 74% (that is, ARISA; fig. S4A). The principal source of variability was associated with the differences in CO_2 flux and associated parameters (table S6).

Benthic invertebrate communities

Total meiofauna density was much higher at REF than at the vented sites [1019 ± 354 individuals (Ind.) m^{-2} versus 407 ± 237 Ind. m^{-2}], which was mirrored in all taxa: nematodes (Fig. 3B) and copepods, which dominated, but also nauplii, polychaetes, and tardigrades (table S7). Total meiofauna and nematode abundances decreased rapidly along the sediment profile (ANOVA; $P < 0.001$; $F_{3,71} = 19.0$ and $F_{3,71} = 11.6$, respectively), more steeply at the CO_2-vented sites than at REF. At REF, this gradient was not reflected in nematode biomass, conversely at CO_2-vented sites, the biomass was significantly higher in the top layer (0 to 2 cm) than in the other layers (ANOVA; $P < 0.001$; $F_{3,20} = 6.6$ for CO2-G and $F_{3,20} = 12.7$ for CO2-R). Community structure for meiofauna at the higher taxon level differed significantly between the three sites (tables S6 and S7) but was even more different at the nematode species level (table S7 and Fig. 4B). Year-to-year differences in the nematode

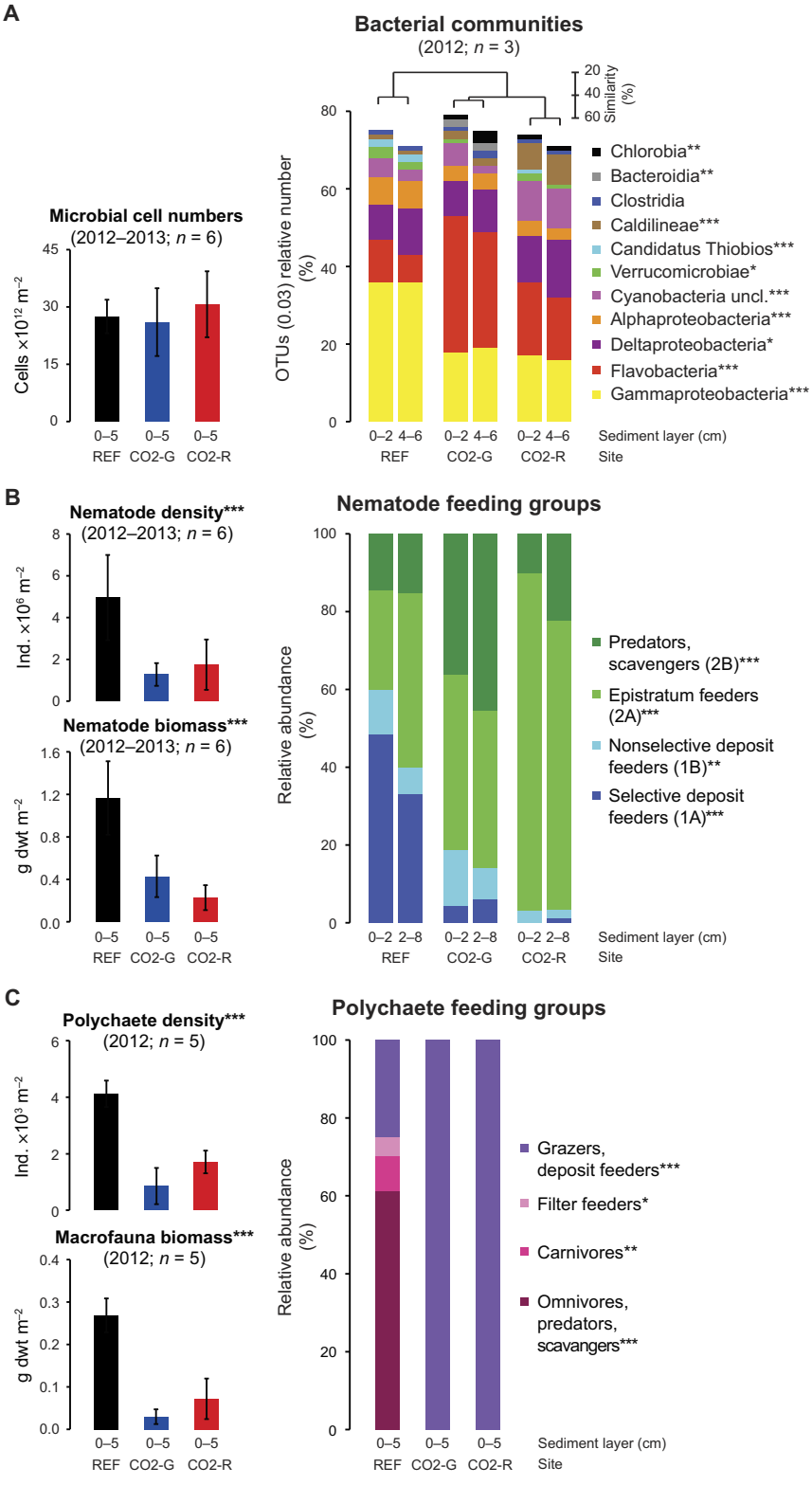

Fig. 3. Community composition of studied sampling site (top 5 cm of sediments). (**A**) Microbial cell numbers and bacterial community structure, as described by 454 MPTS, showing relative number of sequences for dominant bacterial classes (that is, OTUs > 0.1%) clustered according to similarity [based on the Bray-Curtis distance matrix, surface, and subsurface layer; analysis of similarities (ANOSIM); $R = 0.948$; $P < 0.001$]. (**B**) Nematode density and biomass and relative abundance of nematode feeding groups. (**C**) Polychaete density, macrofauna biomass, and relative abundance of polychaete feeding groups. Error bars are ±SD; year and number of sampling are given in each plot; stars indicate significant differences between one or both CO_2-vented sites and the REF (ANOVA; *$P < 0.05$, **$P < 0.01$, ***$P < 0.001$; for details, see table S2E). Ind., individuals; dwt, dry weight; uncl., unclassified.

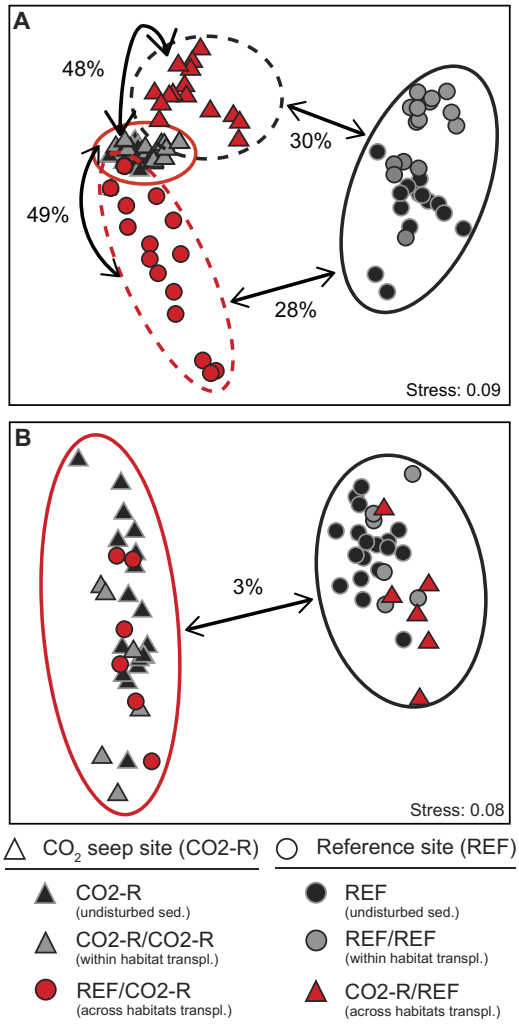

Fig. 4. Effect of medium-term transplantations on benthic community composition. Nonmetric multidimensional scaling ordination plot (based on the Bray-Curtis dissimilarity matrix) of bacterial (ARISA-OTUs–based) and nematode (genus level) community structure for undisturbed sediment (sed.), within-habitat, and across-habitat transplants (transpl.). (**A**) Bacterial community of REF sediment (top, 10-cm layer) transplanted into CO2-R sediment (REF/CO2-R) was significantly different from the source community after 1 year (ANOSIM; $R = 0.982$; $P < 0.001$). The bacterial community of CO2-R transplanted into REF sediment (CO2-R/REF) was also significantly different to that of the original site (ANOSIM; $R = 0.961$; $P < 0.001$). Both communities that were transplanted within their own habitat remained similar to the undisturbed ones. (**B**) Nematode community of the 0- to 4-cm sediment horizon 1 year after transplantation was significantly different in across-habitat transplants (ANOSIM; $R = 0.723$; $P < 0.001$).

community structure at each site accounted for only 8.1% of the variance and could be explained by shifts in relative abundance of the three dominating species at each site, together explaining 40 to 80% of the annual variance (table S6). Most dominant species at REF (that is, >5% relative abundance; table S7) occurred also at the vented sites, but only with <0.5%. Instead, *Microlaimus compridus*, *Microlaimus honestus*, and *Oncholaimus campylocercoides* became highly dominant at both vent sites with >8% (table S7). Generally, the most abundant nematode species at vent sites were rare at REF (0.05 to 0.17% relative abundance). The abundance of selective deposit feeders (1A) decreased at the vent sites, which were instead dominated by predators and scavengers (2B; CO2-G) or epistratum feeders (2A; CO2-R; Fig. 3B). This finding is in line with the highest diatom densities at CO2-R. pH was the most influencing environmental parameter for the nematode assemblage structure over the whole sediment profile, explaining more than 40% of the variance (table S5A).

Macrofauna was dominated by polychaetes at all sites, with relative abundances of 71 ± 8% (REF), 69 ± 45% (CO2-G), and 45 ± 36% (CO2-R). Polychaete abundances, as well as the whole macrobenthos biomass, were substantially lower at the vent sites compared to REF (Fig. 3C). The polychaete community structure also differed significantly between REF and the two vent sites (tables S6 and S7 and fig. S4C). At the vent sites, all polychaetes were grazers or deposit feeders, whereas at REF, filter feeders, carnivores, and omnivores also occurred (Fig. 3C).

Sediment transplantation

Sediment was transplanted between REF and CO2-R, and after 1 year, sediment parameters, microbial activities, nematode density, and bacterial and nematode community structure were compared. In REF/CO2-R, porewater DIC, TA, silicate, and iron increased, and pH decreased, whereas the opposite trend occurred in CO2-R/REF (fig. S3 and table S8). Both pH and carbonate content of CO2-R/REF remained significantly lower than those of REF after 1 year (table S8 and Table 1). Still, the carbonate content increased 35-fold in the 0- to 2-cm sediment layer and doubled in the 4- to 6-cm sediment layer. In contrast, carbonates dissolved in REF/CO2-R both in the 0- to 2-cm sediment layer and in the 4- to 6-cm sediment layer (table S8).

As to microbial activities, the β-glucosidase activity increased in REF/CO2-R, whereas aminopeptidase and esterase activities decreased (fig. S3). SRR also decreased in REF/CO2-R and did not recover in CO2-R/REF (fig. S3). Chl a increased in REF/CO2-R and decreased somewhat in CO2-R/REF (fig. S3).

It took a year until the cross-transplanted bacterial and nematode communities resembled the respective background communities (Fig. 4). However, the nematode density decreased significantly in REF/CO2-R but did not increase in CO2-R/REF (fig. S3). pH and DIC were the main environmental factors responsible for the observed shifts in bacterial and nematode community structure in the transplanted sediments (fig. S5B).

DISCUSSION

Here, we focused on permeable sandy marine ecosystems that occupy large areas of the continental shelves, the target areas for submarine CCS (*7*). To assess potential ecological risks from CO_2 leakage (*5*), we synchronously investigated the geochemical phenomena of CO_2 leakage and its effects on community function and composition including different benthic size classes and trophic groups from microbes to macrofauna. Moreover, our multidisciplinary integrated approach allowed us to test the main hypothesis derived from a meta-analysis of previous experimental and in situ studies (Table 3): CO_2 leakage locally enhances primary production in sandy sediments, but it negatively affects ecosystem functional diversity, with consequences for the benthic food web and carbon fluxes.

Geochemical phenomena of CO_2 venting

Here, we compared the geochemical characteristics of a nonvented REF, representing the natural baseline, with two different CO_2-vented sites, CO2-R and CO2-G, of similar hydrological and sedimentological characteristics (Table 1 and fig. S1). CO_2 leakage was identified visually as

Table 3. Summary of CO_2 impact on benthic organisms and processes at the Basiluzzo Islet sites (soft sediments) and comparison with available benthic data from other shallow natural CO_2 vents (soft and rocky seafloor) at Ischia, Vulcano, and Papua New Guinea. Significant deviations from the REF are described by upward (enhancing) or downward (declining) arrows, respectively, or by + for changes in community structure. 0, neutral; PNG, Papua New Guinea; OC, organic carbon; EEA, extracellular enzymatic activity; Undist., undisturbed sediments at CO_2 vents; Transpl., medium-term (1 year) transplanted sediments from reference to CO_2-impacted site (REF/CO2-R). For references and detailed description of CO_2 affects on marine environments at natural CO_2 vents, see table S9.

		Basiluzzo		Ischia	Vulcano	PNG
		Undist.	Transpl.			
Invertebrates	Community structure	+	+	+	na	+
	Abundance	↓	↓	↑↓	na	↓
	Biomass	↓	na	na	↓	↓
Seagrass	Density	0	na	↑/0	↓	↑
	Biomass	na	na	na	↓	↑
	Photosynthetic activity	na	na	0	↑	↑
Macroalgae	Community structure	na	na	+	na	+
	Community structure	+	na	na	+	na
Microphytobenthos	Abundance	↑	na	na	↑	na
	Biomass	↑	↑	na	↑	na
Bacteria	Community structure	+	+	na	+	+
	Abundance	0	0	na	na	na
Primary production and OC remineralization	Oxygen production	↑	na	na	na	na
	Oxygen respiration	↑	na	na	na	na
	SRR	↓	↓	na	na	na
OC degradation	β-glucosidase (EEA)	↑	↑	na	na	na
	Esterase (EEA)	↓	↓	na	na	na
Nutrients flux	Silicate, iron	↑	↑	na	na	na

escaping gas bubbles of >90% CO_2 content (fig. S1D). Similar to this natural analog, CO_2 upward migration through subseafloor sediment strata in the case of CCS leakage would result in the dissolution of the gas, leading to subsequent reactions with porewater and sediments, so that only a fraction of the gas would escape to the water column (*17*). As a consequence of CO_2 dissolution, porewater pH and carbonate saturation would decrease, whereas DIC and TA will increase (*18*). We recorded all of these geochemical phenomena at the Basiluzzo vent sites: CO_2 venting through the sandy sediments resulted in a loss of solid-phase carbonate and a decrease in porewater pH (Table 1, Fig. 1B, and table S1), as well as in emission of acidified porewaters to the water column (Fig. 1A and table S3). Hence, the long-term geochemical consequence of CO_2 leakage through marine sediments would be the local decline of buffering capacity and a reduction of the mineral carbon sink (Fig. 5).

The CO_2-enriched porewater fluids at Basiluzzo did not contain elevated sulfide or methane concentrations typically associated with hydrothermalism. Boron, found at high concentrations in Panarea hydrothermal fluids (*19*), showed typical seawater concentrations in the Basiluzzo porewaters. The temperature anomaly in the surface sediments at the vent sites was negligible. However, we recorded some ORP dynamics in the bottom water above the vents, as well as substantially elevated iron, manganese, and silicate concentrations in the porewaters, derived from subseafloor hydrothermal and/or CO_2 reactions with the bedrock and overlying sands. Together with the high CO_2 fluxes, these high iron and silicate concentrations apparently enhanced productivity of the microphytobenthos. In an analog CCS leakage scenario, the CO_2 co-leakage will depend on the type of geological reservoir, and these could include mineral products of weathering from CO_2 exposure as well as hydrocarbons (*18*).

Effects of CO_2 venting on primary production and microphytobenthos

The CO_2-vented sites had higher microphytobenthos standing stocks, higher Chl a content, and more TOC, mostly due to an enhanced productivity of benthic diatoms (Figs. 2 and 5), especially where CO_2 leakage was the highest (CO2-R). This effect was reproduced by transplantation of reference sands to CO2-R, showing increased Chl a content after 1 year (fig. S3). Noncalcifying benthic primary producers are likely to profit from high CO_2 (Table 3) as a result of the reduction in the energy costs for carbon concentration mechanisms (*20*). In addition, the higher availability of nutrients (especially silicate and iron, but also phosphorus) in

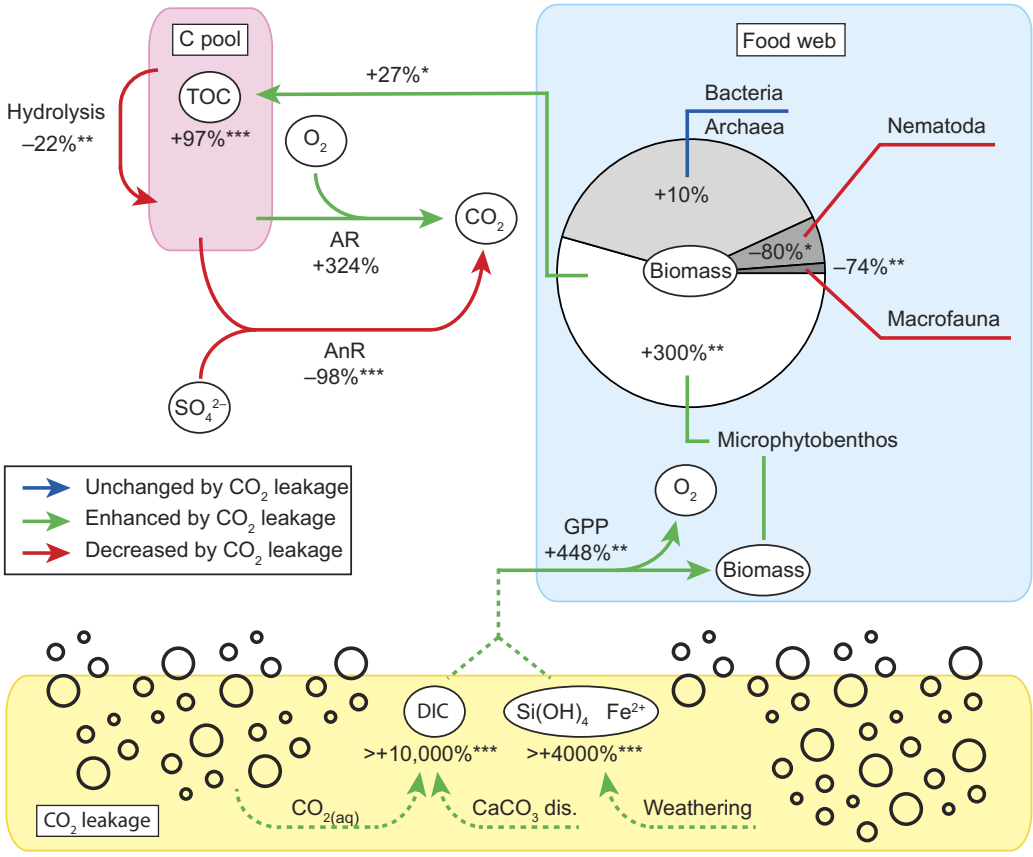

Fig. 5. Synthesis scheme summarizing the effects of CO_2 leakage on the benthic food web. Values depict the percentage of increased or decreased standing stock or activity in CO_2-vented sediments relative to REF [(CO2-R/REF) − 1]. Continuous and dashed arrows show biotic and abiotic processes, respectively. C pool, detrital carbon pool; AR, aerobic respiration; AnR, anaerobic respiration; GPP, gross primary production; $CaCO_3$ dis., $CaCO_3$ dissolution. *P < 0 .05, **P < 0.01, ***P < 0.001 (Welch's t test; n = 3 to 6). Average data of 2012 and 2013 sampling campaigns are shown, except for macrofauna/polychaete data, which are the average of 2012, and for AR and GPP data, which are the average of 2013.

the upward migrating fluids at the vent sites may stimulate microphytobenthos growth. Similar effects were recorded previously along a natural CO_2 gradient at Volcano Island (Italy), where the microphytobenthos was found to be promoted by CO_2 leakage, showing a twofold increase in Chl a concentrations and a two to four times higher diatom abundance under high CO_2 (*21*). As to specific effects on benthic diatom genera, a previous study at Basiluzzo (*22*) suggested that the diatom genera *Fragilaria*, *Diploneis*, and *Amphora* are favored by CO_2 leakage. *Fragilaria* was the most abundant diatom taxon at CO2-R and was observed to form colonies on the surface sands, likely as a response to the combination of CO_2 and nutrient enrichment by porewater advection. This dominance of chain-forming diatoms at CO_2 vent sites has been also reported in other coastal areas (*21*, *23*). Furthermore, *Diploneis* seems to be an opportunistic genus that becomes more competitive in the presence of environmental stress (*24*). This genus, as well as members of *Amphora*, was represented by larger cells with heavily silicified frustules at CO2-R, compared to REF. This increase in microphytobenthos standing stock was also reflected in significantly higher oxygen production at CO2-R compared to REF (Table 2). The CO_2 leakage caused a higher primary production to respiration ratio, keeping more carbon fixed in microphytobenthos biomass and in total organic carbon. Our results suggest that this effect is also due to reduced grazing pressure and altered microbial community function, as discussed below.

Effects on faunal community biomass and composition

Our study shows that CO_2 leakage led to a significant decline in abundance and biomass and a change in community composition for meiofauna and macrofauna (Fig. 3, B and C). Being the most abundant taxa at all target sites, nematodes and polychaetes were particularly affected (fig. S4, B and C). Previous studies using benthic mesocosms and laboratory experiments found that acute CO_2 leakage exposure changed macrofaunal or meiofaunal community abundance, biomass, and composition as a result of seawater acidification (duration of experiments, maximum of 20 weeks; pH levels, ≥5.6) (*11*, *25*–*28*). Specific experiments focusing on nematode communities found no negative effects on abundance, composition, or diversity at pH ≥ 6 (*28*–*30*). For this highly abundant meiofaunal taxon, decreases in density (*29*, *31*, *32*) or an increasing mortality based on changed morphometrics (*33*) only occurred when seawater pH is <6. In our study of naturally CO_2-vented sands, we detected substantial long-term effects on nematodes already below a porewater pH of 7. This effect was reproduced by the experimental transplantations, which lead to a significant decrease of nematode density and a shift in community structure as a direct consequence of CO_2 leakage (fig. S3 and Fig. 3B). The nematode community did not fully recover to background density within 1 year. Furthermore, for several taxa of meiofauna and macrofauna, we show that these CO_2 effects persist under long-time exposure and are not overcome by adaptation and community change. Our results confirm

previous findings on epibenthic macrofauna communities from other CO_2 vents (Table 3) and indicate that few invertebrate taxa can cope with high CO_2. Particularly, opportunistic species with short life spans and capable of rapid colonization in strongly disturbed habitats seemed to tolerate the extreme and chronic high partial pressure of CO_2/low-pH conditions. These include polychaete species of the *Capitella* clade, some spionids, the interstitial hesionid *Microphthalmus tyrrhenicus*, the paraonid *Aricidea cerrutii*, and the nematode species *Microlaimus compridus*, *Microlaimus honestus*, *Oncholaimus campylocercoides*, and *Daptonema microspiculum*. The polychaete and nematode communities also showed a strong trophic shift, being more diversified under the baseline pH conditions (Fig. 3, B and C). Hence, our observations confirm that despite the additional energy availability due to the high microphytobenthic production at the CO_2-vented sites, the associated benthic communities are negatively affected by high CO_2, with declining densities and loss of functional diversity as main consequences.

Effects of elevated CO_2 levels on microbial communities

In contrast to the faunal communities, we did not detect a significant change of bacterial or archaeal densities in CO_2-vented sands compared to REF (Fig. 3A). Some bacterial taxa, like Oceanospirillaceae, did not show differences in relative sequence abundance between vent and REFs and, hence, seem not to be affected by CO_2 leakage (table S4). However, we detected an overall substantial shift in community composition already at the phylum and class levels, which was increasingly pronounced at increasing taxonomic resolution (fig. S4A). Previous studies using natural leakage analogs also found impacts on both microbial compositions already at pH < 7.7 (Table 3).

Here, the most striking change in community composition was the decline of relative abundances of Gammaproteobacteria by 50%. Members of this group typically dominate marine sediments but seem unable to cope well with high CO_2, as previously reported from pelagic mesocosms (*34*–*37*), sedimentary CO_2 vents (*38*, *39*), and sponge and coral associates (*40*). In contrast, the Flavobacteriaceae, a bacterial family relevant in the degradation of marine algal organic matter (*41*), are not negatively affected by high-CO_2 exposure and low pH according to our study, as well as to laboratory experiments (*34*, *42*) and previous observations on natural CO_2-vented sites (*40*, *43*). As for the anaerobic bacteria inhabiting the deeper, more acidified sediments, the Caldilineales, a group involved in organic matter degradation under anaerobic and low-pH conditions (*44*, *45*), were favored at the vented sites. Conversely, the relative sequence numbers of anaerobic bacteria, including sulfate reducers (order Desulfobacterales) and nitrifiers (genus *Nitrospira*, *Nitrospina*, and *Nitrosococcus*), decreased significantly at the CO_2 vents. Despite the high Fe^{2+} availability in porewaters, no mats of iron-oxidizing bacteria were observed, and typical iron oxidizers were missing in the acidified sands. In the transplantations, the significant shift in bacterial community occurring after 1 year (Fig. 4A) was in line with the long-term changes but was not detectable in short-term incubations (that is, 2 weeks; data not shown). Transplantation from the vent site to the REF showed incomplete recovery within a year.

Consequences of CO_2 leakage on local food webs and carbon fluxes

Acidification influences all cellular processes, including enzyme kinetics and membrane potentials, but different species are differently adapted to high CO_2 levels. Our study shows significant, long-lasting effects of high CO_2 on benthic biomass and composition, which alter biogeochemical functions at the ecosystem level (Fig. 5). Integrated with findings from previous experiments and field studies, we prove that these are consistent indicators of high-CO_2 effects across different ecosystem types, organism size classes, and ecological functions.

Our study detected a substantial increase in microphytobenthos primary production and standing stock in relation to CO_2 seepage and the comigration of nutrients such as silicate and iron. We expected this to compensate the metabolic costs of adaptation to high CO_2 for the infaunal communities (*46*), thus favoring high faunal biomasses of a few adapted types. Instead, both meiofauna and macrofauna communities significantly declined in biomass (that is, by up to 90%). Although replacement of typical species of shallow sandy sediments by opportunistic species with different trophic functionalities occurred (Fig. 3, B and C), this did not lead to similar levels of faunal density and biomass. Furthermore, we found a long-lasting shift in microbial community composition and function. The high-CO_2 venting caused a decrease in the whole hydrolytic capacity of the benthic communities, as revealed by measurements of the potential activity of aminopeptidases and esterases (Fig. 2 and fig. S3). These results match those on coastal sediments in mesocosms (*47*). Only the β-glucosidase responded by increased hydrolytic activities, as reported in previous experiments with bacterioplankton (*48*–*51*) and here also with transplant experiments. This enzyme, responsible for polysaccharide degradation, may be enhanced as a consequence of the higher microphytobenthic productivity (*22*). Furthermore, anaerobic remineralization by sulfate reducers was almost fully repressed in the vented sites (Fig. 2 and fig. S3), matching the substantial decline in sulfate reducer sequences. A sensitivity of sulfate-reducing bacteria to high CO_2 was also previously observed at CO_2-vented sediments off Papua New Guinea (*52*). Other functional groups affected by CO_2 based on relative sequence abundance were sulfite oxidizers and nitrifiers.

Together, the observed CO_2-leakage effects had consequences on carbon remineralization per biomass (R/B). This ratio was higher in the vented sands, indicating that more organic carbon needs to be remineralized per unit of biomass, compared to the reference (Table 3 and Fig. 5). Similarly, an altered food web structure and an impaired carbon cycling have been recently reported for soils affected by natural CO_2 leakages (*53*). The results of the transplantation were in full accordance with the observed field patterns, showing basic CO_2 effects on community biomass, composition, and biogeochemical function that will not be overcome by long-term adaptation of the involved species. Rather, the selection of opportunistic or tolerant species caused long-term deviation from reference ecosystem-level functions in terms of productivity, standing stock, and remineralization rates. There was an overall increase of productivity but also a higher respiration rate per standing stock, thus decreasing the biological carbon sink function. Furthermore, the quantitatively more relevant geochemical carbon sink was weakened by the carbonate dissolution and by the long-term loss of buffering capacity due to CO_2 leakage.

CONCLUSION

Our study shows that CO_2 leakage substantially changed the carbonate chemistry in permeable sandy sediments, increasing mineral weathering and nutrient flux (for example, iron and silicate). This led to local shifts in bacterial communities and enhanced microphytobenthos growth but also to a decline in benthic meiofauna and macrofauna density and composition. Together, CO_2 leakage altered the ecosystem functions in terms of remineralization and carbon transfer along the food web. Hence, there is a substantial risk that CO_2 leakage from submarine CCS sites may locally lead to negative impacts on the ecosystem and the function

of the seafloor as carbon sink, when globally, it would help mitigate the detrimental consequences of climate change and acidification on ocean ecosystems. CO_2 leakage from submarine CCS would be very difficult, if not impossible, to stop. Therefore, site selection and spatial planning for marine CCS should include the environmental assessment of habitats, community composition, and ecological functions, including the resilience of local marine species, to mitigate ecological risks.

MATERIALS AND METHODS

Site selection

Locations with natural subseafloor CO_2 venting are studied as analogs to assess the impacts of CO_2 leakage as a risk of CCS technology for marine ecosystems (*12*). Natural CO_2-vented sediments occur in active volcanic/tectonic regions and are driven by hydrothermal circulations (*12*). The selection of purely CO_2-vented sediments for studies of high-CO_2 effects is crucial to reduce confounding factors, such as presence of gases representing microbial energy sources (that is, H_2, H_2S, and CH_4), toxic elements (that is, metals), and temperature anomalies (*54*, *55*). For example, some of the Mediterranean CO_2 vents, such as the one in Levantine Bay of Volcano Island and some at Panarea, show high temperatures around 95°C and a relatively high H_2S gas content of ca. 2%, complicating the isolation of pure CO_2 effects at venting sites by favoring growth of extremophilic and thiotrophic microbial communities (*56*, *57*). Before our study, we evaluated different CO_2-vented habitats around Panarea Island to choose appropriate study sites for investigating the pure effects of CO_2 leakage and seawater acidification on benthic life. During the first expedition (29 May to 10 June 2011), nine gas emission sites and two potential REFs were explored by diving in water depths of around 20-m depth. Larger areas were surveyed by manta towing (*58*). The divers sampled sediments and water asf for pH and sulfide measurements, measured temperature, and took documentary pictures and videos. At the study sites off Basiluzzo Islet, shallow sand flats were interspersed with seagrass meadows at 14- to 21-m depth. The CO_2-impacted sites studied here were identified visually by the ebullition of CO_2 from the seafloor. We found the east of Basiluzzo Islet to be suitable as a submarine natural analog to assess biogeochemical and ecological consequences of CO_2 leakage because of the purity of the gas escaping from the seafloor, combined with the absence of cofounding hydrothermal effects altering microbial communities (Table 1). The experimental fieldwork was carried out in 2012 (02 to 21 June) and 2013 (01 to 14 June).

Data analysis

pH as a key variable for high CO_2 is presented in pH_T. We calibrated all sensors with commercial National Bureau of Standards buffers and corrected these to pH_T by subtracting 0.13 units, as described in Zeebe and Wolf-Gladrow (*59*). To assess significant differences between two or more independent data sets across the different sites, we used Welch's *t* test (for example, sensors network and metadata analysis) or different ANOVAs (for example, biogeochemical and microbiological data and functional groups) (for details, see Statistical Analyses in the Supplementary Materials and Methods).

Chemical analyses of vent gases and fluids, seawater, porewater, and sediments

Gases, seawater, and vent fluids

Gas bubbles were sampled by scuba divers using exetainers and gas-collecting tubes made from glass, and analyzed via gas chromatography for CO_2, O_2, Ar, N_2, CH_4, C_2H_6, C_3H_8, COS, SO_2, and H_2. Hydrogen sulfide concentrations of these bubbles were determined by electrochemical sensor measurements directly after sampling (for details, see the Supplementary Materials). Seawater was sampled with a 5-liter Niskin bottle at ca. 30 cm asf and with 50-ml glass syringes at 5 to 10 cm asf. Benthic chamber water samples (that is, mixture of overlying bottom water and porewater) were collected with 50-ml glass syringes directly connected to benthic chambers at different times and analyzed for pH, nutrient [NH_4^+, PO_4^{3-}, NO_2^-, NO_3^-+NO_2^-, and $Si(OH)_4$] concentration, DIC, and TA. Samples for CH_4 concentration in porewaters were filled into evacuated and preweighed glass containers with 2 to 3 NaOH pellets for subsequent analysis via gas chromatography (Focus GC, Thermo Fisher Scientific) (*60*).

Porewater and sediment geochemistry

Profiles of pH, DIC, TA, and nutrient [NH_4^+, PO_4^{3-}, NO_2^-, NO_3^-+NO_2^-, and $Si(OH)_4$], sulfide, and Fe/Mn concentrations in the sediments were assessed by extracting porewater at 2-cm depth intervals with a TUBO device and with Rhizons (SMS type MOM, 19.21.21F; mean pore size, 0.15 μm; Rhizosphere Research Products) attached to 10-ml syringes. From three replicate push cores per site and per year, samples (2-cm intervals, maximum length up to 10 cm) were preserved for analyses of granulometry, porosity, TOC, TN, CPE (including Chl a), and calcium carbonate ($CaCO_3$) content. The samples were preserved and analyzed as described in Böer *et al.* (*61*) (for details, see the Supplementary Materials). Chl a concentrations were converted to microphytobenthos biomass using a 1:40 Chl a–to–C biomass ratio (*62*).

In situ measurements

Time-lapse recordings

To monitor gas flow visually in situ, time-lapse photography was conducted (videos available at https://doi.pangaea.de/10.1594/PANGAEA.825241) (for details, see the Supplementary Materials).

Oceanographic measurements

A SEAGUARD recording current meter (Aanderaa Data Instruments) was used in 2011, 2012, and 2013 to monitor for 24 to 72 hours current velocity, temperature, salinity/conductivity, pressure, turbidity, and oxygen concentrations within the water column at about 30 cm asf.

Bottom water chemistry loggers

At five selected sites, the pH, oxygen (O_2), ORP, and pressure (tides) were measured using five RBR loggers (RBR-Datalogger XR-420 D; RBR; www.rbr-global.com) with the sensors at 2 cm asf.

Porewater chemistry

A sediment microsensor profiler was equipped with sensors for pH (Microelectrodes Inc.) (*63*), O_2 (*64*), $CO_{2(aq)}$ (Microelectrodes Inc.), ORP (a Pt wire, exposed tip is 50 μm thick and 0.5 mm long), temperature (Pt100; UST Umweltsensortechnik GmbH), H_2 (Unisense), and H_2S (*65*). The profiler was deployed at CO2-R, CO2-G, and REF in 2012. The CO_2 sensors were damaged during the measurement at ca. 2 cm bsf at CO2-R; all other sensors worked successfully.

Diffusive oxygen fluxes

Diffusive oxygen fluxes were calculated from the in situ oxygen microprofiles using Fick's law of diffusion as described previously (*66*).

Total oxygen uptake rates

Benthic chambers were inserted into the seafloor to measure total fluxes of oxygen, nutrients, pH, and DIC within a defined sediment and seawater volume. At CO_2-vented sites, the chambers were deployed between bubble streams to avoid the formation of internal headspace. We repeatedly subsampled the overlying water with syringes during daylight from transparent and masked chambers to assess

oxygen exchange (net O_2 flux) and oxygen respiration, respectively. Oxygen production, that is, gross primary production (GPP), was estimated as net O_2 flux + (O_2 respiration). To correct for anoxic fluid efflux from the seafloor, bags were attached to each chamber to measure the cumulative incubation volume (further information in the Supplementary Materials). Because of relatively high respiration rates, only incubations <6 hours were used to calculate oxygen fluxes.

Sulfate reduction rates

SRRs, as a proxy of anaerobic microbial respiration, were measured ex situ on sediments collected with push corers and sliced in 2-cm intervals (*67*).

Extracellular enzymatic activities

EEAs were analyzed by incubating the top 2 cm of the sediments with substrates for β-glucosidase, chitobiase, leucine aminopeptidase, and esterase (see further details in the Supplementary Materials) (*61*).

Calcite dissolution rates (marble tiles)

The corrosion of $CaCO_3$ structures by CO_2 was determined from the weight loss of marble tiles exposed at 0.5 m asf at REF CO2-G and CO2-R from June 2012 to June 2013. Once retrieved, the marble tiles were dried and weighed, and the dissolution rates were estimated as the difference in weight between pre- and postdeployment tiles, divided by exposure time (362 to 364 days; for further details, see the Supplementary Materials).

Microbiological analyses

Sample collection and DNA extraction

Samples from 0 to 2 cm bsf were obtained by 20 Sarstedt tubes (50 ml), and three push cores were collected for additional sections between 0 and 10 cm bsf per site and per year. Samples were kept frozen at −20°C until subsequent analyses. DNA was extracted from 1 g of sediment per sample using the FastDNA SPIN Kit for Soil (Qbiogene), including an additional heating step to increase yield and final elution of the DNA in tris-EDTA buffer.

Bacterial community structure

The high-throughput fingerprinting technique ARISA [according to Ramette (*68*)] was applied to all sediment samples (0 to 2 cm bsf layer, $n = 23$; 2 to 4 cm, 4 to 6 cm, 6 to 8 cm, and 8 to 10 cm bsf layers, $n = 3$, per site and per year). In addition, 454 MPTS [according to Sogin *et al.* (*69*)] was used for the 0 to 2 and 4 to 6 cm bsf layers collected in 2012 ($n = 3$) (for details, see the Supplementary Materials).

Total microbial and microphytobenthos cell counts

Sediment samples were fixed in 2% (for microbes) and 4% (for microphytobenthos) buffered formaldehyde/seawater and stored at 4°C until subsequent analysis. Microbial abundance was estimated by epifluorescence microscopy after staining with acridine orange (*61*). Catalyzed reporter deposition fluorescence in situ hybridization was applied for bacterial and archaeal cell enumeration. For microphytobenthos, only viable cells were counted under an inverted light microscope (Leica Microsystems AG) using 32× to 40× objective (final magnification, ×320 to ×400) (see the Supplementary Materials).

Fauna sampling and analysis

Meiofauna samples (size class, 0.032 to 1 mm) were collected with precut (2-cm horizons) and taped push cores with an inner diameter of 4.7 cm in 2011 ($n = 3$ per site; upper 8 cm) or 5 cm in 2012 and 2013 ($n = 3$ per site; upper 8 cm). Samples were fixed and preserved in 4% buffered formaldehyde/seawater. Macrofauna samples (size class, >1 mm) were collected with push corers (inner diameter of 6.4 cm; $n = 5$ per site; upper 5 cm). Meiofauna and macrofauna organisms were identified to phylum or class level under a stereoscopic microscope. All meiofaunal nematodes and macrofaunal polychaetes were further identified to species level and allocated to functional feeding groups (see the Supplementary Materials). Depending on reproduction rate and tolerance to disturbance, nematodes were also allocated to a colonizer-persister (cp) category based on Bongers *et al.* (*70*): cp-2, short generation time, high reproduction rate, and very tolerant to disturbances; cp-3, characteristics intermediate to cp-2 and cp-4 and relatively sensitive to disturbances; cp-4, long generation time and sensitive to pollutants; and cp-5, long life span, low reproduction rate, and very sensitive to pollutants and other disturbances. The nematodes' maturity index was determined as an ecological measure of environmental disturbance (see the Supplementary Materials) (*70*).

Sediment transplantation experiments

Sediments were transplanted in situ within and between REF and CO2-R sites: (i) reimplanted at the same site (within habitat: REF/REF and CO2-R/CO2-R) to control for transplantation effects, and (ii) reimplanted to the other habitat type (across habitat: REF/CO2-R and CO2-R/REF) to assess the effect of the different environmental setting. Samples for microbial community analyses (that is, ARISA) were collected immediately after transplantation ($n = 3$ per treatment), after 2 weeks ($n = 1$ per treatment), and after 1 year ($n = 3$ per treatment). Samples for porewater composition, sediment geochemistry, microbial activity, and nematode abundance and community structure were collected 1 year after transplantation ($n = 3$ per treatment). Samples were taken and analyzed as described in the above sections, except for nematodes that were identified at genus level.

SUPPLEMENTARY MATERIALS

Supplementary material for this article is available at http://advances.sciencemag.org/cgi/content/full/4/2/eaao2040/DC1

Supplementary Materials and Methods

fig. S1. Maps and seafloor images of the sampling area.

fig. S2. Bottom water and porewater chemistry.

fig. S3. Biogeochemistry of medium-term transplants and undisturbed sediments.

fig. S4. Similarity between benthic communities at investigated sites.

table S1. Bottom water and porewater chemistry at the study sites off Basiluzzo Islet.

table S2. Outcome of one-way ANOVA.

table S3. pH_T change and in situ fluxes obtained from benthic chambers deployed in 2013.

table S4. Change in relative sequence number of highly abundant, putative functional groups of bacteria based on 454 MPTS OTUs annotation (OTU > 0.1%).

table S5. Outcome of distance-based multivariate regression analysis.

table S6. Outcome of permutational ANOVA for environmental variables (Env. Setting), bacterial community structure (ARISA), and fauna community structure (that is, nematode species, meiofauna higher taxon, polychaete species, and macrofauna higher taxon).

table S7. Relative abundances of macrofauna taxa, polychaete species, meiofauna taxa, and nematode species at the three investigated sites.

table S8. Differences in porewater and sedimentary environmental settings in medium-term transplant experiments ($n = 3$).

table S9. Overview of CO_2/pH impacts on benthic organisms at natural CO_2 vents, as observed in previous studies.

References (*72*–*160*)

REFERENCES AND NOTES

1. H.-O. Pörtner, D. M. Karl, P. W. Boyd, W. W. L. Cheung, S. E. Lluch-Cota, Y. Nojiri, D. N. Schmidt, P. O. Zavialov, Ocean systems, in *Climate Change 2014: Impacts, Adaptation, and Vulnerability. Part A: Global and Sectoral Aspects. Contribution of Working Group II to the Fifth Assessment Report of the Intergovernmental Panel on Climate Change*, C. B. Field, V. R. Barros, D. J. Dokken, K. J. Mach, M. D. Mastrandrea, T. E. Bilir, M. Chatterjee, K. L. Ebi, Y. O. Estrada, R. C. Genova, B. Girma, E. S. Kissel, A. N. Levy, S. MacCracken, P. R. Mastrandrea, L. L.White, Eds. (Cambridge Univ. Press, 2014), pp. 411–484.

2. J.-P. Gattuso, K. J. Mach, G. Morgan, Ocean acidification and its impacts: An expert survey. *Clim. Change* **117**, 725–738 (2013).
3. IEA, Energy and Climate Change. *World Energy Outlook Special Report* (WEO2015), 15 June 2015.
4. S. Holloway, Storage of fossil fuel-derived carbon dioxide beneath the surface of the Earth. *Annu. Rev. Energy Environ.* **26**, 145–166 (2001).
5. J. Blackford, J. M. Bull, M. Cevatoglu, D. Connelly, C. Hauton, R. H. James, A. Lichtschlag, H. Stahl, S. Widdicombe, I. C. Wright, Marine baseline and monitoring strategies for carbon dioxide capture and storage (CCS). *Int. J. Greenh. Gas Control.* **38**, 221–229 (2015).
6. H. A. Botnen, A. M. Omar, I. Thorseth, T. Johannessen, G. Alendal, The effect of submarine CO_2 vents on seawater: Implications for detection of subsea carbon sequestration leakage. *Limnol. Oceanogr.* **60**, 402–410 (2015).
7. D. G. Jones, S. E. Beaubien, J. C. Blackford, E. M. Foekema, J. Lions, C. De Vittor, J. M. West, S. Widdicombe, C. Hauton, A. M. Queirós, Developments since 2005 in understanding potential environmental impacts of CO_2 leakage from geological storage. *Int. J. Greenh. Gas Control.* **40**, 350–377 (2015).
8. S. Widdicombe, S. Dupont, M. Thorndyke, Experimental design of perturbation experiments Laboratory experiments and benthic mesocosm studies, in *Guide to best Practices for Ocean Acidification Research and Data Reporting*, U. Riebesell, V. J. Fabry, L. Hansson, J.-P. Gattuso, Eds. (Publications Office of the European Union, 2010), pp. 113–122.
9. J. Blackford, H. Stahl, J. M. Bull, B. J. P. Bergès, M. Cevatoglu, A. Lichtschlag, D. Connelly, R. H. James, J. Kita, D. Long, M. Naylor, K. Shitashima, D. Smith, P. Taylor, I. Wright, M. Akhurst, B. Chen, T. M. Gernon, C. Hauton, M. Hayashi, H. Kaieda, T. G. Leighton, T. Sato, M. D. J. Sayer, M. Suzumura, K. Tait, M. E. Vardy, P. R. White, S. Widdicombe, Detection and impacts of leakage from sub-seafloor deep geological carbon dioxide storage. *Nat. Clim. Change* **4**, 1011–1016 (2014).
10. J.-P. Gattuso, A. Magnan, R. Bille, W. W. L. Cheung, E. L. Howes, F. Joos, D. Allemand, L. Bopp, S. R. Cooley, C. M. Eakin, O. Hoegh-Guldberg, R. P. Kelly, H.-O. Pörtner, A. D. Rogers, J. M. Baxter, D. Laffoley, D. Osborn, A. Rankovic, J. Rochette, U. R. Sumaila, S. Treyer, C. Turley, Contrasting futures for ocean and society from different anthropogenic CO_2 emissions scenarios. *Science* **349**, aac4722 (2015).
11. S. Widdicombe, C. L. McNeill, H. Stahl, P. Taylor, A. M. Queirós, J. Nunes, K. Tait, Impact of sub-seabed CO_2 leakage on macrobenthic community structure and diversity. *Int. J. Greenh. Gas Control.* **38**, 182–192 (2015).
12. F. Inagaki, M. M. M. Kuypers, U. Tsunogai, J.-i. Ishibashi, K.-i. Nakamura, T. Treude, S. Ohkubo, M. Nakaseama, K. Gena, H. Chiba, H. Hirayama, T. Nunoura, K. Takai, B. B. Jørgensen, K. Horikoshi, A. Boetius, Microbial community in a sediment-hosted CO_2 lake of the southern Okinawa Trough hydrothermal system. *Proc. Natl. Acad. Sci. U.S.A.* **103**, 14164–14169 (2006).
13. J. M. Sunday, K. E. Fabricius, K. J. Kroeker, K. M. Anderson, N. E. Brown, J. P. Barry, S. D. Connell, S. Dupont, B. Gaylord, J. M. Hall-Spencer, T. Klinger, M. Milazzo, P. L. Munday, B. D. Russell, E. Sanford, V. Thiyagarajan, M. L. H. Vaughan, S. Widdicombe, C. D. G. Harley, Ocean acidification can mediate biodiversity shifts by changing biogenic habitat. *Nat. Clim. Change* **7**, 81–85 (2017).
14. M. Huettel, P. Berg, J. E. Kostka, Benthic exchange and biogeochemical cycling in permeable sediments. *Ann. Rev. Mar. Sci.* **6**, 23–51 (2014).
15. G. Gabbianelli, P. Y. Gillot, G. Lanzafame, C. Romagnoli, P. L. Rossi, Tectonic and volcanic evolution of Panarea (Aeolian Islands, Italy). *Mar. Geol.* **92**, 313–326 (1990).
16. F. Gamberi, M. Marani, C. Savelli, Tectonic, volcanic and hydrothermal features of a submarine portion of the Aeolian arc (Tyrrhenian Sea). *Mar. Geol.* **140**, 167–181 (1997).
17. M. Cevatoglu, J. M. Bull, M. E. Vardy, T. M. Gernon, I. C. Wright, D. Long, Gas migration pathways, controlling mechanisms and changes in sediment acoustic properties observed in a controlled sub-seabed CO_2 release experiment. *Int. J. Greenh. Gas Control.* **38**, 26–43 (2015).
18. A. Lichtschlag, R. H. James, H. Stahl, D. Connelly, Effect of a controlled sub-seabed release of CO_2 on the biogeochemistry of shallow marine sediments, their pore waters, and the overlying water column. *Int. J. Greenh. Gas Control.* **38**, 80–92 (2015).
19. F. Tassi, B. Capaccioni, G. Caramanna, D. Cinti, G. Montegrossi, L. Pizzino, F. Quattrocchi, O. Vaselli, Low-pH waters discharging from submarine vents at Panarea Island (Aeolian Islands, southern Italy) after the 2002 gas blast: Origin of hydrothermal fluids and implications for volcanic surveillance. *Appl. Geochem.* **24**, 246–254 (2009).
20. B. M. Hopkinson, C. L. Dupont, A. E. Allen, F. M. M. Morel, Efficiency of the CO_2-concentrating mechanism of diatoms. *Proc. Natl. Acad. Sci. U.S.A.* **108**, 3830–3837 (2011).
21. V. R. Johnson, C. Brownlee, M. Milazzo, J. Hall-Spencer, Marine microphytobenthic assemblage shift along a natural shallow-water CO_2 gradient subjected to multiple environmental stressors. *J. Mar. Sci. Eng.* **3**, 1425–1447 (2015).
22. M. Rogelja, T. Cibic, C. Pennesi, C. De Vittor, Microphytobenthic community composition and primary production at gas and thermal vents in the Aeolian Islands (Tyrrhenian Sea, Italy). *Mar. Environ. Res.* **118**, 31–44 (2016).
23. V. R. Johnson, C. Brownlee, R. E. M. Rickaby, M. Graziano, M. Milazzo, J. M. Hall-Spencer, Responses of marine benthic microalgae to elevated CO_2. *Mar. Biol.* **160**, 1813–1824 (2013).
24. T. Cibic, C. Comici, A. Bussani, P. Del Negro, Benthic diatom response to changing environmental conditions. *Estuar. Coast. Shelf Sci.* **115**, 158–169 (2012).
25. S. Widdicombe, S. L. Dashfield, C. L. McNeill, H. R. Needham, A. Beesley, A. McEvoy, S. Øxnevad, K. R. Clarke, J. A. Berge, Effects of CO_2 induced seawater acidification on infaunal diversity and sediment nutrient fluxes. *Mar. Ecol. Prog. Ser.* **379**, 59–75 (2009).
26. R. Hale, P. Calosi, L. Mcneill, N. Mieszkowska, S. Widdicombe, Predicted levels of future ocean acidification and temperature rise could alter community structure and biodiversity in marine benthic communities. *Oikos* **120**, 661–674 (2011).
27. N. Christen, P. Calosi, C. L. McNeill, S. Widdicombe, Structural and functional vulnerability to elevated pCO_2 in marine benthic communities. *Mar. Biol.* **160**, 2113–2128 (2013).
28. H. Schade, L. Mevenkamp, K. Guilini, S. Meyer, S. N. Gorb, D. Abele, A. Vanreusel, F. Melzner, Simulated leakage of high pCO_2 water negatively impacts bivalve dominated infaunal communities from the Western Baltic Sea. *Sci. Rep.* **6**, 31447 (2016).
29. K. Takeuchi, Y. Fujioka, Y. Kawasaki, Y. Shirayama, Impacts of high concentration of CO_2 on marine organisms; a modification of CO_2 ocean sequestration. *Energy Convers. Manage.* **38**, S337–S341 (1997).
30. S. L. Dashfield, P. J. Somerfield, S. Widdicombe, M. C. Austen, M. Nimmo, Impacts of ocean acidification and burrowing urchins on within-sediment pH profiles and subtidal nematode communities. *J. Exp. Mar. Biol. Ecol.* **365**, 46–52 (2008).
31. J. P. Barry, T. Tyrrell, L. Hansson, G.-K. Plattner, J.-P. Gattuso, Experimental design of perturbation experiments, in *Guide to best Practices for Ocean Acidification Research and Data Reporting*, U. Riebesell, V. J. Fabry, L. Hansson, J.-P. Gattuso, Eds. (Publications Office of the European Union, Luxembourg, 2010), pp. 53–136.
32. H. Ishida, Y. Watanabe, T. Fukuhara, S. Kaneko, K. Furusawa, Y. Shirayama, In situ enclosure experiment using a benthic chamber system to assess the effect of high concentration of CO_2 on deep-sea benthic communities. *J. Oceanogr.* **61**, 835–843 (2005).
33. J. W. Fleeger, D. S. Johnson, K. R. Carman, P. B. Weisenhorn, A. Gabriele, D. Thistle, J. P. Barry, The response of nematodes to deep-sea CO_2 sequestration: A quantile regression approach. *Deep Sea Res. Part I Oceanogr. Res. Pap.* **57**, 696–707 (2010).
34. E. Krause, A. Wichels, L. Giménez, M. Lunau, M. B. Schilhabel, G. Gerdts, Small changes in pH have direct effects on marine bacterial community composition: A microcosm approach. *PLOS ONE* **7**, e47035 (2012).
35. A.-S. Roy, S. M. Gibbons, H. Schunck, S. Owens, J. G. Caporaso, M. Sperling, J. I. Nissimov, S. Romac, L. Bittner, U. Riebesell, J. LaRoche, J. A. Gilbert, Ocean acidification shows negligible impacts on high-latitude bacterial community structure in coastal pelagic mesocosms. *Biogeosci. Discuss.* **9**, 13319–13349 (2012).
36. A. Monier, H. S. Findlay, S. Charvet, C. Lovejoy, Late winter under ice pelagic microbial communities in the high Arctic Ocean and the impact of short-term exposure to elevated CO_2 levels. *Front. Microbiol.* **5**, 490 (2014).
37. A. Chauhan, A. Pathak, R. Rodolfo-Metalpa, M. Milazzo, S. J. Green, J. M. Hall-Spencer, Metagenomics reveals planktonic bacterial community shifts across a natural CO_2 gradient in the Mediterranean Sea. *Genome Announc.* **3**, e01543-14 (2015).
38. K. Yanagawa, Y. Morono, D. de Beer, M. Haeckel, M. Sunamura, T. Futagami, T. Hoshino, T. Terada, K.-i. Nakamura, T. Urabe, G. Rehder, A. Boetius, F. Inagaki, Metabolically active microbial communities in marine sediment under high-CO_2 and low-pH extremes. *ISME J.* **7**, 555–567 (2013).
39. D. Kerfahi, J. M. Hall-Spencer, B. M. Tripathi, M. Milazzo, J. Lee, J. M. Adams, Shallow water marine sediment bacterial community shifts along a natural CO_2 gradient in the Mediterranean Sea off Vulcano, Italy. *Microb. Ecol.* **67**, 819–828 (2014).
40. K. M. Morrow, D. G. Bourne, C. Humphrey, E. S. Botté, P. Laffy, J. Zaneveld, S. Uthicke, K. E. Fabricius, N. S. Webster, Natural volcanic CO_2 seeps reveal future trajectories for host-microbial associations in corals and sponges. *ISME J.* **9**, 894–908 (2015).
41. J. P. Bowman, The marine clade of the family *Flavobacteriaceae*: The genera *Aequorivita*, *Arenibacter*, *Cellulophaga*, *Croceibacter*, *Formosa*, *Gelidibacter*, *Gillisia*, *Maribacter*, *Mesonia*, *Muricauda*, *Polaribacter*, *Psychroflexus*, *Psychroserpens*, *Robiginitalea*, *Salegentibacter*, *Tenacibaculum*, *Ulvibacter*, *Vitellibacter* and *Zobellia*. *Prokaryotes Vol.* **7**, 677–694 (2006).
42. E. Teira, A. Fernández, X. A. Álvarez-Salgado, E. E. García-Martín, P. Serret, C. Sobrino, Response of two marine bacterial isolates to high CO_2 concentration. *Mar. Ecol. Prog. Ser.* **453**, 27–36 (2012).
43. F. F. Raulf, K. Fabricius, S. Uthicke, D. de Beer, R. M. M. Abed, A. Ramette, Changes in microbial communities in coastal sediments along natural CO_2 gradients at a volcanic vent in Papua New Guinea. *Environ. Microbiol.* **17**, 3678–3691 (2015).
44. T. Yamada, Y. Sekiguchi, S. Hanada, H. Imachi, A. Ohashi, H. Harada, Y. Kamagata, *Anaerolinea thermolimosa* sp. nov., *Levilinea saccharolytica* gen. nov., sp. nov. and *Leptolinea tardivitalis* gen. nov., sp. nov., novel filamentous anaerobes, and description

of the new classes *Anaerolineae* classis nov. and *Caldilineae* classis nov. in the bacterial phylum. *Int. J. Syst. Evol. Microbiol.* **56**, 1331–1340 (2006).
45. A. Schippers, D. Kock, C. Höft, G. Köweker, M. Siegert, Quantification of microbial communities in subsurface marine sediments of the Black Sea and off Namibia. *Front. Microbiol.* **3**, 16 (2012).
46. S. L. Garrard, M. C. Gambi, M. B. Scipione, F. P. Patti, M. Lorenti, V. Zupo, D. M. Paterson, M. C. Buia, Indirect effects may buffer negative responses of seagrass invertebrate communities to ocean acidification. *J. Exp. Mar. Bio. Ecol.* **461**, 31–38 (2014).
47. E. Rastelli, C. Corinaldesi, A. Dell'Anno, T. Amaro, S. Greco, M. Lo Martire, L. Carugati, A. M. Queirós, S. Widdicombe, R. Danovaro, CO_2 leakage from carbon dioxide capture and storage (CCS) systems affects organic matter cycling in surface marine sediments. *Mar. Environ. Res.* **122**, 158–168 (2016).
48. H.-P. Grossart, M. Allgaier, U. Passow, U. Riebesell, Testing the effect of CO_2 concentration on the dynamics of marine heterotrophic bacterioplankton. *Limnol. Oceanogr.* **51**, 1–11 (2006).
49. J. Piontek, M. Lunau, N. Händel, C. Borchard, M. Wurst, A. Engel, Acidification increases microbial polysaccharide degradation in the ocean. *Biogeosciences* **7**, 1615–1624 (2010).
50. T. J. Burrell, E. W. Maas, P. Teesdale-Spittle, C. S. Law, Optimising methodology for determining the effect of ocean acidification on bacterial extracellular enzymes. *Biogeosciences Discuss.* **12**, 5841–5870 (2015).
51. M. M. Sala, F. L. Aparicio, V. Balagué, J. A. Boras, E. Borrull, C. Cardelús, L. Cros, A. Gomes, A. López-Sanz, A. Malits, R. A. Martínez, M. Mestre, J. Movilla, H. Sarmento, E. Vázquez-Domínguez, D. Vaqué, J. Pinhassi, A. Calbet, E. Calvo, J. M. Gasol, C. Pelejero, C. Marrasé, Contrasting effects of ocean acidification on the microbial food web under different trophic conditions. *ICES J. Mar. Sci.* **73**, 670–679 (2016).
52. C. Hassenruck, A. Fink, A. Lichtschlag, H. E. Tegetmeyer, D. De Beer, A. Ramette, Quantification of the effects of ocean acidification on sediment microbial communities in the environment: The importance of ecosystem approaches. *FEMS Microbiol. Ecol.* **92**, fiw027 (2016).
53. F. Beulig, T. Urich, M. Nowak, S. E. Trumbore, G. Gleixner, G. D. Gilfillan, K. E. Fjelland, K. Küsel, Altered carbon turnover processes and microbiomes in soils under long-term extremely high CO_2 exposure. *Nat. Microbiol.* **1**, 15025 (2016).
54. F. Wenzhöfer, O. Holby, R. N. Glud, H. K. Nielsen, J. K. Gundersen, In situ microsensor studies of a shallow water hydrothermal vent at Milos, Greece. *Mar. Chem.* **69**, 43–54 (2000).
55. S. Vizzini, R. Di Leonardo, V. Costa, C. D. Tramati, F. Luzzu, A. Mazzola, Trace element bias in the use of CO_2 vents as analogues for low pH environments: Implications for contamination levels in acidified oceans. *Estuar. Coast. Shelf Sci.* **134**, 19–30 (2013).
56. J. P. Amend, K. L. Rogers, E. L. Shock, S. Gurrieri, S. Inguaggiato, Energetics of chemolithoautotrophy in the hydrothermal system of Vulcano Island, southern Italy. *Geobiology* **1**, 37–58 (2003).
57. R. E. Price, D. E. LaRowe, F. Italiano, I. Savov, T. Pichler, J. P. Amend, Subsurface hydrothermal processes and the bioenergetics of chemolithoautotrophy at the shallow-sea vents off Panarea Island (Italy). *Chem. Geol.* **407–408**, 21–45 (2015).
58. S. English, C. Wilkinson, V. Baker, *Survey Manual for Tropical Marine Resources* (Australian Insitute of AMrine Science, ed. 2, 1997).
59. R. Zeebe, D. Wolf-Gladrow, *CO_2 in Seawater-Equilibrium, Kinetics, Isotopes* (Elsevier, 2001).
60. N. M. Thang, V. Brüchert, M. Formolo, G. Wegener, L. Ginters, B. B. Jørgensen, T. G. Ferdelman, The impact of sediment and carbon fluxes on the biogeochemistry of methane and sulfur in littoral Baltic Sea sediments (Himmerfjärden, Sweden). *Estuaries Coast.* **36**, 98–115 (2013).
61. S. I. Böer, C. Arnosti, J. E. E. van Beusekom, A. Boetius, Temporal variations in microbial activities and carbon turnover in subtidal sandy sediments. *Biogeosciences* **6**, 1149–1165 (2009).
62. P. J. P. Santos, J. Castel, L. P. Souzasantos, Spatial distribution and dynamics of microphytobenthos biomass in the Gironde estuary (France). *Ocean. Acta* **20**, 549–556 (1997).
63. D. De Beer, A. Glud, E. H. G. Epping, M. Kühl, A fast-responding CO_2 microelectrode for profiling sediments, microbial mats, and biofilms. *Limnol. Oceanogr.* **42**, 1590–1600 (1997).
64. N. P. Revsbech, D. M. Ward, Oxygen microelectrode that is insensitive to medium chemical composition: Use in an acid microbial mat dominated by *Cyanidium caldarium*. *Appl. Environ. Microbiol.* **45**, 755–759 (1983).
65. P. Jeroschewski, C. Steuckart, M. Kuhl, An amperometric microsensor for the determination of H_2S in aquatic environments. *Anal. Chem.* **68**, 4351–4357 (1996).
66. N. P. Revsbech, B. B. Jørgensen, O. Brix, Primary production of microalgae in sediments measured by oxygen microprofile, $H_{14}CO_3$ - fixation, and oxygen exchange methods. *Limnol. Oceanogr.* **26**, 717–730 (1981).
67. J. Kallmeyer, T. G. Ferdelman, A. Weber, H. Fossing, B. B. Jørgensen, A cold chromium distillation procedure for radiolabeled sulfide applied to sulfate reduction measurements. *Limnol. Oceanogr.* **2**, 171–180 (2004).
68. A. Ramette, Quantitative community fingerprinting methods for estimating the abundance of operational taxonomic units in natural microbial communities. *Appl. Environ. Microbiol.* **75**, 2495–2505 (2009).
69. M. L. Sogin, H. G. Morrison, J. A. Huber, D. M. Welch, S. M. Huse, P. R. Neal, J. M. Arrieta, G. J. Herndl, Microbial diversity in the deep sea and the underexplored "rare biosphere". *Proc. Natl. Acad. Sci. U.S.A.* **103**, 12115–12120 (2006).
70. T. Bongers, R. Alkemade, G. W. Yeates, Interpretation of disturbance-induced maturity decrease in marine nematode assemblages by means of the maturity index. *Mar. Ecol. Prog. Ser.* **76**, 135–142 (1991).
71. M. Diepenbroek, F. O. Glöckner, P. Grobe, A. Güntsch, R. Huber, B. König-Ries, I. Kostadinov, J. Nieschulze, B. Seeger, R. Tolksdorf, D. Triebel, Towards an integrated biodiversity and ecological research data management and archiving platform: The German Federation for the Curation of Biological Data (GFBio), in *Informatik 2014 – Big Data Komplexität meistern. GI-Edition: Lecture Notes in Informatics (LNI) – Proceedings*. (Köllen Verlag, 2014), pp. 1711–1724.
72. K. Grasshoff, K. Kremling, M. Ehrhardt, *Methods of Seawater Analysis* (Wiley-VHC, 1983).
73. P. O. J. Hall, R. C. Aller, Rapid small-volume flow injection analysis for ΣCO_2 and NH_4^+ in marine and freshwaters. *Limnol. Oceanogr.* **37**, 1113–1119 (1992).
74. J. M. Edmond, High precision determination of titration alkalinity and total carbon dioxide content of sea water by potentiometric titration. *Deep Sea Res.* **17**, 737–750 (1970).
75. J. D. Cline, Spectrophometric determination of hydrogen sulfide in natural waters. *Limnol. Oceanogr.* **14**, 454–458 (1969).
76. J. W. McLaren, S. S. Berman, V. J. Boyko, D. S. Russell, Simultaneous determination of major, minor, and trace elements in marine sediments by inductively coupled plasma atomic emission spectrometry. *Anal. Chem.* **53**, 1802–1806 (1981).
77. C. K. Wentworth, A scale of grade and class terms for clastic sediments. *J. Geol.* **30**, 377–392 (1922).
78. E. E. Engleman, L. L. Jackson, D. R. Norton, Determination of carbonate carbon in geological materials by coulometric titration. *Chem. Geol.* **53**, 125–128 (1985).
79. J. W. McLaren, D. Beauchemin, S. S. Berman, Determination of trace metals in marine sediments by inductively coupled plasma spectrometry. *J. Anal. At. Spectrom* **2**, 277–281 (1987).
80. P. L. M. Cook, F. Wenzhöfer, R. N. Glud, F. Janssen, M. Huettel, Benthic solute exchange and carbon mineralization in two shallow subtidal sandy sediments: Effect of advective pore-water exchange. *Limnol. Oceanogr.* **52**, 1943–1963 (2007).
81. F. Janssen, M. Huettel, U. Witte, Pore-water advection and solute fluxes in permeable marine sediments (II): Benthic respiration at three sandy sites with different permeabilities (German Bight, North Sea). *Limnol. Oceanogr.* **50**, 779–792 (2005).
82. E. D. Melton, E. D. Swanner, S. Behrens, C. Schmidt, A. Kappler, The interplay of microbially mediated and abiotic reactions in the biogeochemical Fe cycle. *Nat. Rev. Microbiol.* **12**, 797–808 (2014).
83. C. Bienhold, L. Zinger, A. Boetius, A. Ramette, Diversity and biogeography of bathyal and abyssal seafloor bacteria. *PLOS ONE* **11**, e0148016 (2016).
84. S. E. Dowd, T. R. Callaway, R. D. Wolcott, Y. Sun, T. McKeehan, R. G. Hagevoort, T. S. Edrington, Evaluation of the bacterial diversity in the feces of cattle using 16S rDNA bacterial tag-encoded FLX amplicon pyrosequencing (bTEFAP). *BMC Microbiol.* **8**, 125 (2008).
85. P. D. Schloss, S. L. Westcott, T. Ryabin, J. R. Hall, M. Hartmann, E. B. Hollister, R. A. Lesniewski, B. B. Oakley, D. H. Parks, C. J. Robinson, J. W. Sahl, B. Stres, G. G. Thallinger, D. J. Van Horn, C. F. Weber, Introducing mothur: Open-source, platform-independent, community-supported software for describing and comparing microbial communities. *Appl. Environ. Microbiol.* **75**, 7537–7541 (2009).
86. C. Quast, E. Pruesse, P. Yilmaz, J. Gerken, T. Schweer, P. Yarza, J. Peplies, F. O. Glöckner, The SILVA ribosomal RNA gene database project: Improved data processing and web-based tools. *Nucleic Acids Res.* **41**, D590–D596 (2013).
87. K. Ishii, M. Mußmann, B. J. MacGregor, R. Amann, An improved fluorescence in situ hybridization protocol for the identification of bacteria and archaea in marine sediments. *FEMS Microbiol. Ecol.* **50**, 203–213 (2004).
88. M. Molari, E. Manini, Reliability of CARD-FISH procedure for enumeration of archaea in deep-sea surficial sediments. *Curr. Microbiol.* **64**, 242–250 (2012).
89. R. I. Amann, B. J. Binder, R. J. Olson, S. W. Chisholm, R. Devereux, D. A. Stahl, Combination of 16S rRNA-targeted oligonucleotide probes with flow cytometry for analyzing mixed microbial populations. *Appl. Environ. Microbiol.* **56**, 1919–1925 (1990).
90. H. Daims, A. Brühl, R. Amann, K.-H. Schleifer, M. Wagner, The Domain-specific probe EUB338 is insufficient for the detection of all *Bacteria*: Development and evaluation of a more comprehensive probe set. *Syst. Appl. Microbiol.* **22**, 434–444 (1999).
91. D. A. Stahl, R. Amann, Development and application of nucleic acid probes, in *Nucleic Acid Techniques in Bacterial Systematics*, E. Stackebrandt, M. Goodfellow, Eds. (John Wiley & Sons Ltd., 1991), pp. 205–248.
92. R. I. Amann, W. Ludwig, K. H. Schleifer, Phylogenetic identification and in situ detection of individual microbial cells without cultivation. *Microbiol. Rev.* **59**, 143–169 (1995).

93. H. Utermöhl, Zur Vervollkommnung der quantitativen Phytoplankton-Methodik. *Int. Ver. The.* **9**, 1–38 (1958).
94. F. E. Round, R. M. Crawford, D. G. Mann, *The Diatoms: Biology and Morphology of the Genera* (Cambridge Univ. Press, 1990).
95. T. Cibic, O. Blasutto, S. Fonda Umani, Biodiversity of settled material in a sediment trap in the gulf of Trieste (northern Adriatic Sea). *Hydrobiologia* **580**, 57–75 (2007).
96. F. Widdel, F. Bak, Gram-Negative Mesophilic Sulfate-Reducing Bacteria, in *The Prokaryotes*, A. Balows, H. G. Trüper, M. Dworkin, W. Harder, K. H. Schleifer, Eds. (Springer-Verlag, 1992), pp. 3352–3378.
97. J. W. Seinhorst, A rapid method for the transfer of nematodes from fixative to anhydrous glycerin. *Nematologica* **4**, 67–69 (1959).
98. K. Guilini, T. N. Bezerra, U. Eisendle-Flöckner, T. Deprez, G. Fonseca, O. Holovachov, D. Leduc, D. Miljutin, T. Moens, J. Sharma, N. Smol, A. Tchesunov, V. Mokievsky, J. Vanaverbeke, A. Vanreusel, V. Venekey, M. Vincx, *NeMys: World Database of Free-Living Marine Nematodes.* (2017); http://nemys.ugent.be.
99. G. Read, K. Fauchald, *World Polychaeta database* (2016); http://www.marinespecies.org/polychaeta.
100. J. C. F. Gil, The European fauna of Annelida Polychaeta, (Fac. Ciências. Univ. Lisboa, 2011); http://hdl.handle.net/10451/4600.
101. I. Andrassy, The determination of volume and weight of nematodes. *Acta. Zool. Hung.* **2**, 1–15 (1956).
102. C. Heip, M. Vincx, G. Vranken, The ecology of marine nematodes. *Oceanogr. Mar. Biol. Ann. Rev.* **23**, 399–489 (1985).
103. S. Ankar, R. Elmgren, Benthic macro- and meiofauna of the Askö-Landsort area (Northern Baltic Porper): A stratified random sampling survey. *Contrib. Askö Lab.* **11**, 1–115 (1976).
104. B. T. Hargrave, V. E. Kostylev, C. M. Hawkins, Benthic epifauna assemblages, biomass and respiration in The Gully region on the Scotian Shelf, NW Atlantic Ocean. *Mar. Ecol. Prog. Ser.* **270**, 55–70 (2004).
105. W. Wieser, Die beziehung zwischen mundhöhlengestalt, ernährungsweise und vorkommen bei freilebenden marinen nematoden. Eine ökologisch-morphologische studie. *Ark. Zool.* **4**, 439–483 (1953).
106. P. A. Jumars, K. M. Dorgan, S. M. Lindsay, Diet of worms emended: An update of polychaete feeding guilds. *Ann. Rev. Mar. Sci.* **7**, 497–520 (2015).
107. R-Development-Core-Team, *R: A Language and Environment for Statistical Computing*. (R Found. Stat. Comput. Vienna, Austria 2014); http://www.r-project.org/.
108. M. J. Anderson, A new method for non-parametric multivariate analysis of variance. *Austral Ecol.* **26**, 32–46 (2001).
109. B. H. McArdle, M. J. Anderson, Fitting multivariate models to community data: A comment on distance-based redundancy analysis. *Ecology* **82**, 290–297 (2001).
110. K. Clarke, R. N. Gorley, *Primer v6: User Manual/Tutorial* (Plymouth Marine Laboratory, 2006).
111. M. J. Anderson, R. N. Gorley, R. K. Clarke, *PERMANOVA+ for PRIMER: Guide to Software and Statistical Methods* (Plymouth: PRIMER-E Ltd., 2008).
112. R. N. Roy, L. N. Roy, K. M. Vogel, C. Porter-Moore, T. Pearson, C. E. Good, F. J. Millero, D. M. Campbell, The dissociation constants of carbonic acid in seawater at salinities 5 to 45 and temperatures 0 to 45°C. *Mar. Chem.* **44**, 249–267 (1993).
113. DOE, *Handbook of methods for the analysis of the various parameters of the carbon dioxide system in sea water version 2* (1994); http://cdiac.esd.ornl.gov/oceans/DOE_94.pdf.
114. A. G. Dickson, Thermodynamics of the dissociation of boric acid in synthetic seawater from 273.15 to 318.15 K. *Deep. Sea. Res.* **37**, 755–766 (1990).
115. J. M. Hall-Spencer, R. Rodolfo-Metalpa, S. Martin, E. Ransome, M. Fine, S. M. Turner, S. J. Rowley, D. Tedesco, M.-C. Buia, Volcanic carbon dioxide vents show ecosystem effects of ocean acidification. *Nature* **454**, 96–99 (2008).
116. S. Martin, R. Rodolfo-Metalpa, E. Ransome, S. Rowley, M.-C. Buia, J.-P. Gattuso, J. Hall-Spencer, Effects of naturally acidified seawater on seagrass calcareous epibionts. *Biol. Lett.* **4**, 689–692 (2008).
117. M. Cigliano, M. C. Gambi, R. Rodolfo-Metalpa, F. P. Patti, J. M. Hall-Spencer, Effects of ocean acidification on invertebrate settlement at volcanic CO_2 vents. *Mar. Biol.* **157**, 2489–2502 (2010).
118. B. B. Dias, M. B. Hart, C. W. Smart, J. M. Hall-Spencer, Modern seawater acidification: The response of foraminifera to high-CO_2 conditions in the Mediterranean Sea. *J. Geol. Soc. London* **167**, 843–846 (2010).
119. R. Rodolfo-Metalpa, C. Lombardi, S. Cocito, J. M. Hall-Spencer, M. C. Gambi, Effects of ocean acidification and high temperatures on the bryozoan *Myriapora truncata* at natural CO_2 vents. *Mar. Ecol.* **31**, 447–456 (2010).
120. V. Kitidis, B. Laverock, L. C. McNeill, A. Beesley, D. Cummings, K. Tait, M. A. Osborn, S. Widdicombe, Impact of ocean acidification on benthic and water column ammonia oxidation. *Geophys. Res. Lett.* **38**, L21603 (2011).
121. K. J. Kroeker, F. Micheli, M. C. Gambi, T. R. Martz, Divergent ecosystem responses within a benthic marine community to ocean acidification. *Proc. Natl. Acad. Sci. U.S.A.* **108**, 14515–14520 (2011).
122. R. Rodolfo-Metalpa, F. Houlbrèque, É. Tambutté, F. Boisson, C. Baggini, F. P. Patti, R. Jeffree, M. Fine, A. Foggo, J.-P. Gattuso, J. M. Hall-Spencer, Coral and mollusc resistance to ocean acidification adversely affected by warming. *Nat. Clim. Change* **1**, 308–312 (2011).
123. L. Porzio, M. C. Buia, J. M. Hall-Spencer, Effects of ocean acidification on macroalgal communities. *J. Exp. Mar. Bio. Ecol.* **400**, 278–287 (2011).
124. D. Meron, E. Atias, L. Iasur Kruh, H. Elifantz, D. Minz, M. Fine, E. Banin, The impact of reduced pH on the microbial community of the coral *Acropora eurystoma*. *ISME J.* **5**, 51–60 (2011).
125. D. Meron, M.-C. Buia, M. Fine, E. Banin, Changes in microbial communities associated with the sea anemone *Anemonia viridis* in a natural pH gradient. *Microb. Ecol.* **65**, 269–276 (2013).
126. L. Porzio, S. L. Garrard, M. C. Buia, The effect of ocean acidification on early algal colonization stages at natural CO_2 vents. *Mar. Biol.* **160**, 2247–2259 (2013).
127. L. Donnarumma, C. Lombardi, S. Cocito, M. C. Gambi, Settlement pattern of Posidonia oceanica epibionts along a gradient of ocean acidification: An approach with mimics. *Mediterr. Mar. Sci.* **15**, 498–509 (2014).
128. C. Goodwin, R. Rodolfo-Metalpa, B. Picton, J. M. Hall-Spencer, Effects of ocean acidification on sponge communities. *Mar. Ecol.* **35**, 41–49 (2014).
129. E. Ricevuto, K. J. Kroeker, F. Ferrigno, F. Micheli, M. C. Gambi, Spatio-temporal variability of polychaete colonization at volcanic CO_2 vents indicates high tolerance to ocean acidification. *Mar. Biol.* **161**, 2909–2919 (2014).
130. L. Basso, I. E. Hendriks, A. B. Rodríguez-Navarro, M. C. Gambi, C. M. Duarte, Extreme pH Conditions at a natural CO_2 vent system (Italy) affect growth, and survival of juvenile pen shells (*Pinna nobilis*). *Estuaries Coast.* **38**, 1986–1999 (2015).
131. C. Lauritano, M. Ruocco, E. Dattolo, M. C. Buia, J. Silva, R. Santos, I. Olivé, M. M. Costa, G. Procaccini, Response of key stress-related genes of the seagrass *Posidonia oceanica* in the vicinity of submarine volcanic vents. *Biogeosciences Discuss.* **12**, 4947–4971 (2015).
132. C. Lombardi, M. C. Gambi, C. Vasapollo, P. Taylor, S. Cocito, Skeletal alterations and polymorphism in a Mediterranean bryozoan at natural CO_2 vents. *Zoomorphology* **130**, 135–145 (2011).
133. C. Lombardi, S. Cocito, M. C. Gambi, P. D. Taylor, Morphological plasticity in a calcifying modular organism: Evidence from an in situ transplant experiment in a natural CO_2 vent system. *R. Soc. Open Sci.* **2**, 140413 (2015).
134. M. C. Gambi, L. Musco, A. Giangrande, F. Badalamenti, F. Micheli, K. J. Kroeker, Distribution and functional traits of polychaetes in a CO_2 vent system: Winners and losers among closely related species. *Mar. Ecol. Prog. Ser.* **550**, 121–134 (2016).
135. N. M. Lucey, C. Lombardi, M. Florio, L. DeMarchi, M. Nannini, S. Rundle, M. C. Gambi, P. Calosi, An in situ assessment of local adaptation in a calcifying polychaete from a shallow CO_2 vent system. *Evol. Appl.* **9**, 1054–1071 (2016).
136. A. Kumar, I. Castellano, F. P. Patti, M. Delledonne, H. Abdelgawad, G. T. S. Beemster, H. Asard, A. Palumbo, M. C. Buia, Molecular response of *Sargassum vulgare* to acidification at volcanic CO_2 vents: Insights from de novo transcriptomic analysis. *Mol. Ecol.* **26**, 2276–2290 (2017).
137. T. Arnold, C. Mealey, H. Leahey, A. W. Miller, J. M. Hall-Spencer, M. Milazzo, K. Maers, Ocean acidification and the loss of phenolic substances in marine plants. *PLOS ONE* **7**, e35107 (2012).
138. I. Lidbury, V. Johnson, J. M. Hall-Spencer, C. B. Munn, M. Cunliffe, Community-level response of coastal microbial biofilms to ocean acidification in a natural carbon dioxide vent ecosystem. *Mar. Pollut. Bull.* **64**, 1063–1066 (2012).
139. P. Calosi, S. P. S. Rastrick, M. Graziano, S. C. Thomas, C. Baggini, H. A. Carter, J. M. Hall-Spencer, M. Milazzo, J. I. Spicer, Distribution of sea urchins living near shallow water CO_2 vents is dependent upon species acid–base and ion-regulatory abilities. *Mar. Pollut. Bull.* **73**, 470–484 (2013).
140. E. T. Apostolaki, S. Vizzini, I. E. Hendriks, Y. S. Olsen, Seagrass ecosystem response to long-term high CO_2 in a Mediterranean volcanic vent. *Mar. Environ. Res.* **99**, 9–15 (2014).
141. J. D. Taylor, R. Ellis, M. Milazzo, J. M. Hall-Spencer, M. Cunliffe, Intertidal epilithic bacteria diversity changes along a naturally occurring carbon dioxide and pH gradient. *FEMS Microbiol. Ecol.* **89**, 670–678 (2014).
142. V. Garilli, R. Rodolfo-Metalpa, D. Scuderi, L. Brusca, D. Parrinello, S. P. S. Rastrick, A. Foggo, R. J. Twitchett, J. M. Hall-Spencer, M. Milazzo, Physiological advantages of dwarfing in surviving extinctions in high-CO_2 oceans. *Nat. Clim. Change* **5**, 678–682 (2015).
143. P. Ventura, M. D. Jarrold, P.-L. Merle, S. Barnay-Verdier, T. Zamoum, R. Rodolfo-Metalpa, P. Calosi, P. Furla, Resilience to ocean acidification: Decreased carbonic anhydrase activity in sea anemones under high pCO_2 conditions. *Mar. Ecol. Prog. Ser.* **559**, 257–263 (2016).
144. E. Manini, G. M. Luna, C. Corinaldesi, D. Zeppilli, G. Bortoluzzi, G. Caramanna, F. Raffa, R. Danovaro, Prokaryote diversity and virus abundance in shallow hydrothermal vents of the Mediterranean Sea (Panarea Island) and the Pacific Ocean (North Sulawesi-Indonesia). *Microb. Ecol.* **55**, 626–639 (2008).

145. S. Goffredo, F. Prada, E. Caroselli, B. Capaccioni, F. Zaccanti, L. Pasquini, P. Fantazzini, S. Fermani, M. Reggi, O. Levy, K. E. Fabricius, Z. Dubinsky, G. Falini, Biomineralization control related to population density under ocean acidification. *Nat. Clim. Change* **4**, 593–597 (2014).
146. P. Fantazzini, S. Mengoli, L. Pasquini, V. Bortolotti, L. Brizi, M. Mariani, M. Di Giosia, S. Fermani, B. Capaccioni, E. Caroselli, F. Prada, F. Zaccanti, O. Levy, Z. Dubinsky, J. A. Kaandorp, P. Konglerd, J. U. Hammel, Y. Dauphin, J.-P. Cuif, J. C. Weaver, K. E. Fabricius, W. Wagermaier, P. Fratzl, G. Falini, S. Goffredo, Gains and losses of coral skeletal porosity changes with ocean acidification acclimation. *Nat. Commun.* **6**, 7785 (2015).
147. K. Guilini, M. Weber, D. de Beer, M. Schneider, M. Molari, C. Lott, W. Bodnar, T. Mascart, M. De Troch, A. Vanreusel, Response of *Posidonia oceanica* seagrass and its epibiont communities to ocean acidification. *PLOS ONE* **12**, e0181531 (2017).
148. K. E. Fabricius, C. Langdon, S. Uthicke, C. Humphrey, S. Noonan, G. De'ath, R. Okazaki, N. Muehllehner, M. S. Glas, J. M. Lough, Losers and winners in coral reefs acclimatized to elevated carbon dioxide concentrations. *Nat. Clim. Change* **1**, 165–169 (2011).
149. B. D. Russell, S. D. Connell, S. Uthicke, N. Muehllehner, K. E. Fabricius, J. M. Hall-Spencer, Future seagrass beds: Can increased productivity lead to increased carbon storage? *Mar. Pollut. Bull.* **73**, 463–469 (2013).
150. K. E. Fabricius, G. De'ath, S. Noonan, S. Uthicke, Ecological effects of ocean acidification and habitat complexity on reef-associated macroinvertebrate communities. *Proc. Biol. Sci.* **281**, 20132479 (2013).
151. K. E. Fabricius, A. Kluibenschedl, L. Harrington, S. Noonan, G. De'ath, In situ changes of tropical crustose coralline algae along carbon dioxide gradients. *Sci. Rep.* **5**, 9537 (2015).
152. C. Hassenrück, L. C. Hofmann, K. Bischof, A. Ramette, Seagrass biofilm communities at a naturally CO_2-rich vent. *Environ. Microbiol. Rep.* **7**, 516–525 (2015).
153. C. Hassenrück, A. Fink, A. Lichtschlag, H. E. Tegetmeyer, D. de Beer, A. Ramette, Quantification of the effects of ocean acidification on sediment microbial communities in the environment: The importance of ecosystem approaches. *FEMS Microbiol. Ecol.* **92**, fiw027 (2016).
154. S. Uthicke, T. Ebert, M. Liddy, C. Johansson, K. E. Fabricius, M. Lamare, *Echinometra* sea urchins acclimatized to elevated pCO_2 at volcanic vents outperform those under present-day pCO_2 conditions. *Glob. Chang. Biol.* **22**, 2451–2461 (2016).
155. C. Hassenrück, H. E. Tegetmeyer, A. Ramette, K. E. Fabricius, Minor impacts of reduced pH on bacterial biofilms on settlement tiles along natural pH gradients at two CO_2 seeps in Papua New Guinea. *ICES J. Mar. Sci.* **74**, 978–987 (2017).
156. H. C. Barkley, A. L. Cohen, Y. Golbuu, V. R. Starczak, T. M. DeCarlo, K. E. F. Shamberger, Changes in coral reef communities across a natural gradient in seawater pH. *Sci. Adv.* **1**, e1500328 (2015).
157. I. C. Enochs, D. P. Manzello, E. M. Donham, G. Kolodziej, R. Okano, L. Johnston, C. Young, J. Iguel, C. B. Edwards, M. D. Fox, L. Valentino, S. Johnson, D. Benavente, S. J. Clark, R. Carlton, T. Burton, Y. Eynaud, N. N. Price, Shift from coral to macroalgae dominance on a volcanically acidified reef. *Nat. Clim. Change* **5**, 1083–1088 (2015).
158. T. Nunoura, H. Oida, M. Nakaseama, A. Kosaka, S. B. Ohkubo, T. Kikuchi, H. Kazama, S. Hosoi-Tanabe, K.-i. Nakamura, M. Kinoshita, H. Hirayama, F. Inagaki, U. Tsunogai, J.-i. Ishibashi, K. Takai, Archaeal diversity and distribution along thermal and geochemical gradients in hydrothermal sediments at the yonaguni knoll IV hydrothermal field in the Southern Okinawa Trough. *Appl. Environ. Microbiol.* **76**, 1198–1211 (2010).
159. D. de Beer, M. Haeckel, J. Neumann, G. Wegener, F. Inagaki, A. Boetius, Saturated CO_2 inhibits microbial processes in CO_2-vented deep-sea sediments. *Biogeosciences* **10**, 5639–5649 (2013).
160. C. Linares, M. Vidal, M. Canals, D. K. Kersting, D. Amblas, E. Aspillaga, E. Cebrián, A. Delgado-Huertas, D. Díaz, J. Garrabou, B. Hereu, L. Navarro, N. Teixidó, E. Ballesteros, Persistent natural acidification drives major distribution shifts in marine benthic ecosystems. *Proc. Biol. Sci.* **282**, 20150587 (2015).

Acknowledgments: The authors would like to thank B. Merkel (TU Freiberg) for the sediment element analysis in 2011, F. Italiano [Istituto Nazionale di Geofisica e Vulcanologia (INGV) Palermo] for the vent fluid analysis in 2011, S. Beaubien and S. Lombardi (UniRoma1) for the on-site analysis of H_2S gas in 2012, N. Bigalke (GEOMAR) for the estimation of the gas emission rates, M. Haeckel and R. Surberg (GEOMAR) for the porewater element analysis, J. Gil [Centre d'Estudis Avançats de Blanes, Consejo Superior de Investigaciones Cientificas (CEAB-CSIC)] for his help in identifying some problematic polychaetes, and D. Wolf-Gladrow for the helpful discussions of the carbonate system. The authors are also grateful for the technical support by M. Meiners, E. Weiz-Bersch, M. Alisch, W. Stiens, and R. Stiens (HGF-MPG Joint Research Group on Deep Sea Ecology and Technology); help in field work and laboratory activities by N. Viaene, B. Beuselinck, A. Van Kenhove, G. De Smet, F. Sedano Vera, N. De Jesr, and L. Lins (UGent Marine Biology); scientific diving assistance by B. Unger, M. Schneider, H. Kuhfuss, and A. Eich (HYDRA Institute for Marine Sciences); and logistic support by A. Fogliuzzi (Amphibia). **Funding:** This work was funded by the European Union Seventh Framework Programme (FP7/2007-2013) under grant agreement number 265847 [Sub-seabed CO_2 storage: Impact on Marine Ecosystems (ECO2)] and supported by the Max Planck Society and by the Flemish Fund for Scientific Research (grant number 1242114N). This study is also a contribution of D.M. to the research project MarSymBiomics (reference number CTM2013-43287-P), funded by the Spanish "Agencia Estatal de Investigación" (AEI), and PopCOmics (CTM2017-88080), funded by the AEI and the European Funds for Regional Development (FEDER) and to the Consolidated Research Group on Marine Benthic Ecology (2014SGR120) of the Generalitat de Catalunya. **Author contributions:** This study was designed by A.B. and A.R. Sampling activities and in situ experiments were performed by M.W., C.L., K.G., S.M., M.M., D.d.B., F.W., and A.R. M.M., D.d.B., and F.W. analyzed the in situ measurements. M.M. and G.W. analyzed the microbial and biogeochemical data. K.G. and D.M. analyzed the meiofauna and macrofauna. T.C. and C.D.V. analyzed the microphytobenthos. C.L. and M.W. analyzed the videos and images of the study sites. A.B., A.V., D.d.B., and M.W. contributed reagents/materials/analysis tools. The paper was written by M.M., K.G., and A.B. with contributions and final approval of all co-authors. **Competing interests:** The authors declare that they have no competing interests. **Data and materials availability:** All data were archived on the PANGAEA database: doi.pangaea.de/10.1594/PANGAEA.871453. Porewater element composition can be found at doi.pangaea.de/10.1594/PANGAEA.847916, and sediment element composition at doi.pangaea.de/10.1594/PANGAEA.847825. MPTS sequences were deposited on the European Nucleotide Archive under accession number PRJEB21026. The sequences were archived using the brokerage service of the German Federation for Biological Data (*71*). All data needed to evaluate the conclusions in the paper are present in the paper and/or the Supplementary Materials. Additional data related to this paper may be requested from the authors.

Submitted 29 June 2017
Accepted 5 January 2018
Published 7 February 2018
10.1126/sciadv.aao2040

Citation: M. Molari, K. Guilini, C. Lott, M. Weber, D. de Beer, S. Meyer, A. Ramette, G. Wegener, F. Wenzhöfer, D. Martin, T. Cibic, C. De Vittor, A. Vanreusel, A. Boetius, CO_2 leakage alters biogeochemical and ecological functions of submarine sands. *Sci. Adv.* **4**, eaao2040 (2018).

CO_2 leakage alters biogeochemical and ecological functions of submarine sands

Massimiliano Molari, Katja Guilini, Christian Lott, Miriam Weber, Dirk de Beer, Stefanie Meyer, Alban Ramette, Gunter Wegener, Frank Wenzhöfer, Daniel Martin, Tamara Cibic, Cinzia De Vittor, Ann Vanreusel and Antje Boetius

Sci Adv **4** (2), eaao2040.
DOI: 10.1126/sciadv.aao2040